ACS OMEGA

Open Access

This article is licensed under CC-BY-NC-ND 4.0

http://pubs.acs.org/journal/acsodf

Review

The Promise of Metal-Doped Iron Oxide Nanoparticles as Antimicrobial Agent

Nazifa Tabassum Tasnim,‡ Nushrat Ferdous,‡ Md. Mahamudul Hasan Rumon, and Md Salman Shakil*

Cite This: *ACS Omega* 2024, 9, 16−32

Read Online

ACCESS | Metrics & More | Article Recommendations

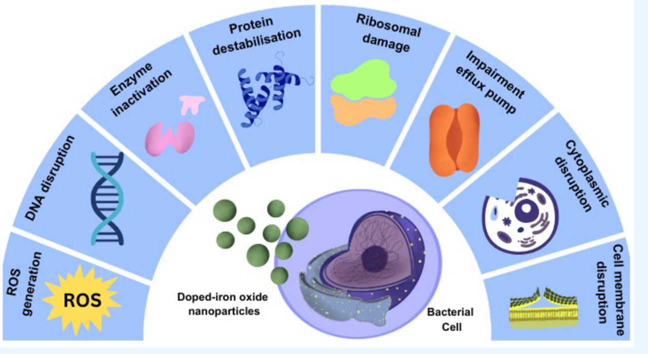

ABSTRACT: Antibiotic resistance (AMR) is one of the pressing global public health concerns and projections indicate a potential 10 million fatalities by the year 2050. The decreasing effectiveness of commercially available antibiotics due to the drug resistance phenomenon has spurred research efforts to develop potent and safe antimicrobial agents. Iron oxide nanoparticles (IONPs), especially when doped with metals, have emerged as a promising avenue for combating microbial infections. Like IONPs, the antimicrobial activities of doped-IONPs are also linked to their surface charge, size, and shape. Doping metals on nanoparticles can alter the size and magnetic properties by reducing the energy band gap and combining electronic charges with spins. Furthermore, smaller metal-doped nanoparticles tend to exhibit enhanced antimicrobial activity due to their higher surface-to-volume ratio, facilitating greater interaction with bacterial cells. Moreover, metal doping can also lead to increased charge density in magnetic nanoparticles and thereby elevate reactive oxygen species (ROS) generation. These ROS play a vital role to disrupt bacterial cell membrane, proteins, or nucleic acids. In this review, we compared the antimicrobial activities of different doped-IONPs, elucidated their mechanism(s), and put forth opinions for improved biocompatibility.

1. INTRODUCTION

Antimicrobial resistance (AMR) is an urgent public health issue associated with severe mortality and morbidity.[1] Nearly 700,000 death occurrences are recorded due to AMR of various types of bacteria, and this statistic is estimated to cross 10 million before the year 2050.[2] Additionally, bacteria acquiring antibiotic resistance gene(s) and developing a wide array of AMR mechanisms to protect them from commercially available antimicrobial agents.[3] Given the severity of drug resistance and the scarcity of therapeutic choices, researchers are developing more efficient and potent antibacterial agents. Recently, nanoparticle-based materials have drawn attention in the treatment of microbial infections.[4−11]

Among the nanosize materials, iron oxide nanoparticles (IONPs) are promising nanoparticles having unique and tunable magnetic properties, excellent biocompatibility, and vast surface to conjugate theranostic moieties.[12,13] IONPs are utilized for magnetic resonance imaging (MRI) contrast dyes,[14] drug delivery vehicles,[15] antimicrobial agents,[16] separating environmental pollutants,[17,18] and sensing and diagnosing disease or pathogens.[19] Interestingly, the conjugation of antibiotics or other antimicrobial agents with IONPs makes them more sensitive to bacteria and help to overcome drug resistance.[20] Furthermore, doping metal atoms can enhance the antimicrobial activity and magnetic properties of IONPs.[21] Doping is the controlled insertion of a foreign element into the unoccupied crystal lattice of different parts to alter their characteristics.[22] Similarly, the insertion of foreign metal particles into IONPs alter their physicochemical, as well as biological, electrical, and optical, properties[22] and improve performance compared to bare IONPs.[23] IONPs are doped with several metals, and their oxides, such as Ni,[24,25] Cu,[26,27] Co,[28] Zn,[29,30] Se,[31] Mo,[32] Au,[33,34] ZnO,[35,36] CuO,[37] exhibit antimicrobial activity toward pathogenic bacteria.

In the past few years, many review articles reported the antimicrobial properties and antimicrobial mechanisms of actions of IONPs. For instance, recently Gudkov et al. (2021)[38] and Arias et al. (2018)[39] discussed the advances in the antimicrobial activity of IONPs against different micro-organisms via a variety of interactions (*e.g.*, generation of ROS, peroxidation of lipids, alterations to DNA, membrane depolarization with ensuing deterioration of the integrity of

Received: August 25, 2023
Revised: November 26, 2023
Accepted: November 29, 2023
Published: December 21, 2023

© 2023 The Authors. Published by American Chemical Society

cell and release of metal ions influencing homeostasis of cells along with coordination of protein) and how biocompatible IONPs were with eukaryotic cells and tissues. Hamdy et al. (2022)[40] also highlighted how the plant-based green-synthesized IONPs could exhibit antimicrobial activities by strongly inhibiting the Gram-positive bacteria and moderately inhibiting the growth of Gram-negative bacteria through ROS, which included hydrogen peroxide (H_2O_2), hydroxyl radicals ($HO^\bullet$), and superoxide anions ($O_2^{\bullet-}$), and could harm biological elements including DNA, proteins, and lipids, as well as bacterial enzymatic processes. Furthermore, Xu et al. (2019)[19] reported that IONPs had potential as prospective platforms for antimicrobial activities and detection of bacterial infection due to their magnetic properties. Recently, Yang et al. (2023)[41] identified the limitation of IONPs (*e.g.*, agglomeration, lower magnetic relativity, insufficient functionality). Moreover, authors also summarized various synthesis methods to control size, shape, or properties of IONPs and highlighted different biomedical applications including antimicrobial activity.[41] However, it was worth noting that Gudkov et al. (2021),[38] Hamdy et al. (2022),[40] and Yang et al. (2023)[41] did not report the influence of the doping metals on the physical properties of IONPs, comparative analysis of antimicrobial activities of different metal-doped IONPs, antimicrobial mechanism of action(s) and approaches to improve biocompatibility of different metal doped-IONPs.

In this perspective, we scrutinized the antimicrobial activities of metal-doped IONPs and their potential mechanism(s) of action against pathogenic bacteria. Additionally, we pointed out the different effects of stimuli and the potential pitfalls of metals as doping agents and proposed future directions to improve the biocompatibility of doped-IONPs.

2. IONPS

Ferrimagnetic IONPs are utilized in numerous applications of biomedical and bioengineering.[42] Different polymorphic forms of iron oxides, such as γ-Fe_2O_3, Fe_3O_4, and FeO, which are, respectively, maghemite, magnetite, and wustite. Among these, γ-Fe_2O_3 and Fe_3O_4 are widely explored from of IONPs due to their special properties including high specific surface area, superparamagnetism, and biocompatibility.[43] At nanoscale dimension, quantum phenomena influence the optical, electrical, and magnetic properties of matter.[44−46]For instance, magnetic Fe_3O_4 nanoparticles with 3−50 nm in size are superparamagnetic.[47] An elevated surface area-to-volume ratio permits efficient dispersion in solution form thereby rendering these materials optimal for surface functionalization and modification in an extensive spectrum of uses, including magnetic sorting, sensing, separation techniques, hyperthermia, drug delivery, etc.[48,49]

3. DOPED-IRON OXIDE NANOPARTICLES (DOPED-IONPS)

Doped-IONPs are composed of modified iron oxides by introducing foreign metals or elements into their structure.[25,28,36,50−52] Introduction of foreign metals, also known as dopants, into an empty crystal lattice alters the physicochemical, biological, electrical, as well as optical properties of the nanoparticles.[22] Doped-IONPs can be synthesized by coprecipitation (CP), green combustion (GC), sol−gel process (SGP), chemical polymerization approach (CPA), microwave-assisted process (MAP), hydrothermal approach (HDA).[24,25,28,34,36,50−52] Multiple types of dopants, *e.g.*, cobalt, nickel, copper, zinc, and rare-earth elements are broadly applied for doping purposes.[23,24,26,28,29] At present, doped-IONPs have found widespread applications in drug delivery, antimicrobial and anticancer activities, MRI imaging agent.[53−56] Moreover, when doped-IONPs are employed as antimicrobial agents, transition metals are mainly utilized due to their antimicrobial characteristics in their bulk form.[31]

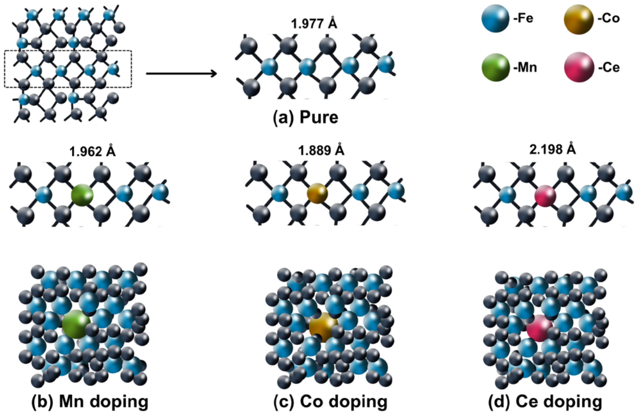

Figure 1. Structures of the γ-Fe_2O_3(001) lattice with various TMISs (Mn(II), Co(II), and Ce(IV)), (a) pure, (b) Mn-doped γ-Fe_2O_3, (c) Co-doped γ-Fe_2O_3, and (d) Ce-doped γ-Fe_2O_3 (navy blue: lose electrons, emerald green: obtain electron). The idea of the diagram is taken from Xie et al. (2021).[76]

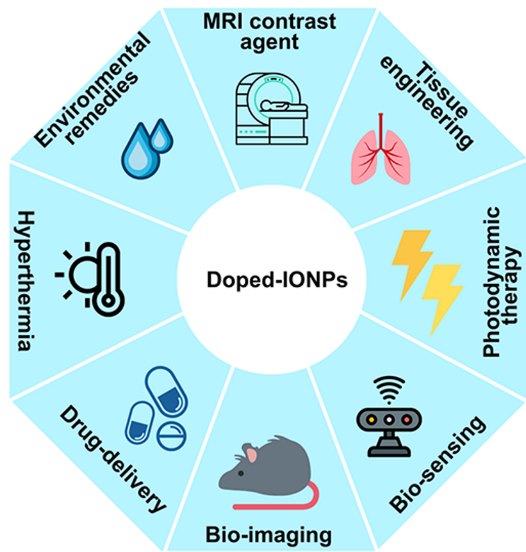

Figure 2. Schematic representation of various applications of doped-IONPs. Doped-IONPs have been utilized in MRI, visualization and diagnostics, cancer therapy employing magnetic hyperthermia, photodynamic therapy, bioimaging, biosensor development, environmental remedies, and tissue engineering. MRI: Magnetic resonance imaging.

Incorporating transition metals into IONPs exhibited higher antimicrobial activity than bare IONPs.[57] Casula et al. (2016)[58] stated that the bare IONPs can obtain intrinsic magnetic properties and desired morphological or structural features by doping. This modification could potentially enhance the antimicrobial activity of doped-IONPs.[59] Aghari et al. (2013)[31] also demonstrated that doped-IONPs yield

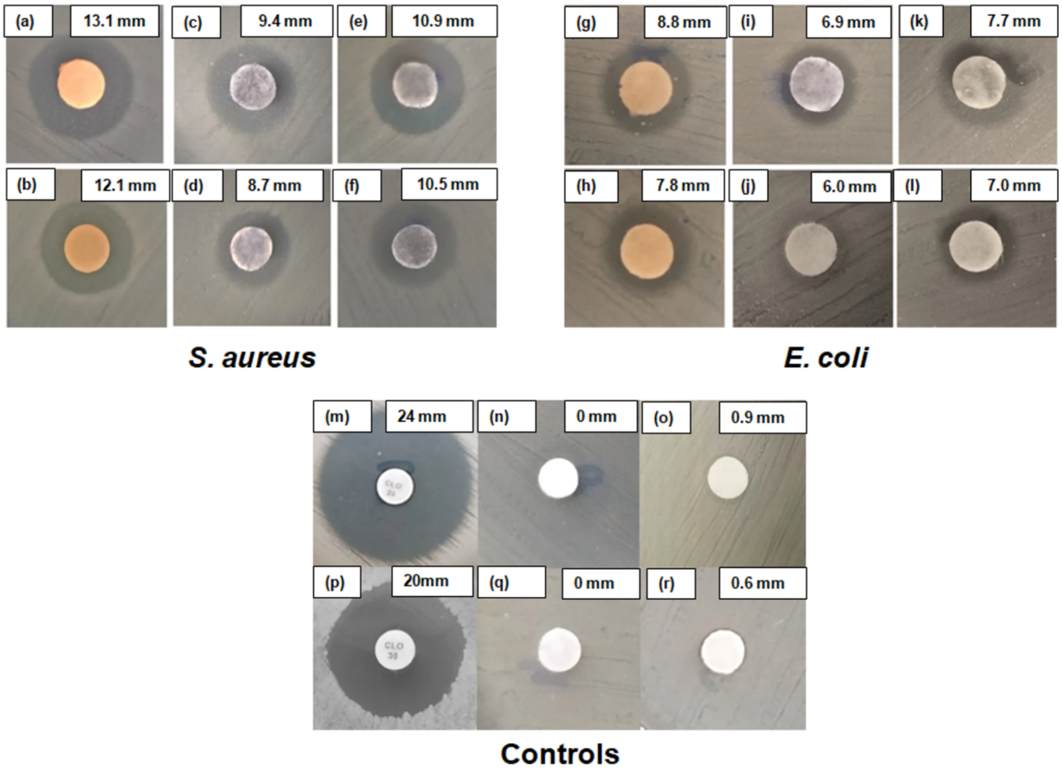

Figure 3. ZOI (mm) of doped-IONPs against *S. aureus* and *E. coli* by disk diffusion method. ZOI of $ZnFe_2O_4$ calcined at 250 °C (a), and 800 °C (b). $CoFe_2O_4$ calcined at 250 °C (c), and 800 °C (d). $Zn_{0.5}Co_{0.5}Fe_2O_4$ calcined at 250 °C (e), and 800 °C (f) against *S. aureus*.ZOI of $ZnFe_2O_4$ calcined at 250 °C (g), and 800 °C (h). $CoFe_2O_4$ calcined at 250 °C (i), and 800 °C (j), and $Zn_{0.5}Co_{0.5}Fe_2O_4$ calcined at 250 °C (k) and 800 °C (l) against *E. coli*. Disk diffusion test for strains of *S. Aureus* (m−o) and *E. coli* (p−r), and ZOI of the controls. (m, p) Chloramphenicol; (n, q) negative control (distilled water); and (o, r) dispersion control (nanoemulsion). Gram-positive bacteria (*S. aureus*) exhibited larger ZOI than Gram-negative bacteria (E. coli). Additionally, a lower calcination temperature (250 °C) demonstrated larger ZOI than a higher temperature (800 °C). Image adapted from Morais et al. (2021)[114] which is under Creative Commons Attribution 4.0 International License (http://creativecommons.org/licenses/by/4.0/, accessed on 1 August 2023). This License permits adaptation, distribution, and reproduction in any medium or format as long as you give appropriate credit to the original author(s). ZOI: Zone of inhibition.

more than bare IONPs. However, careful consideration of the dopant type and concentration is necessary to achieve desired nanoparticles without compromising their functionality.[60]

3.1. Biocatalytic Activity of Doped-IONPs.

The biocatalytic activity of IONPs is linked to their application as theranostic agents. This process can be modulated through modification of their fundamental structure.[61] However, their effectiveness as biocatalysts in the biomedical field remains uncertain since of their modest conductivity and larger band gap.[62,63]Enhancement of the electronic configuration and number of biologically active sites is an efficient approach for boosting their electrical conductivity as well as chemical−physical aspects enabling biocatalysis since these factors play a significant influence on catalytic performances.[64,65]Numerous techniques are aimed at improving a material's catalytic effectiveness by offering a greater abundance of catalytic sites with an expanded surface area, such as the inclusion of additional substances or doping defect technology, the architecture of composite materials, and so on.[66,67]Among these, doping is a practical approach to augmenting the efficiency of biocatalytic processes through the incorporation of additional atoms within the mother metal oxide lattice structure. After successfully doping, the dopant can regulate the electronic configuration of the biocatalyst by boosting the electric charge carrier density and conductivity and further improving the active sites.[68] Several studies have already broadly discussed various doping techniques. However, there has been limited discussion on the effective doping mechanism of iron-based composite biocatalysts.[69] This section will provide an overview of the mechanistic discussion associated with the various transition metals doped on IONPs.

Recently, heterogeneous magnetic IONPs MFe_2O_4, where the transition metal(s) is denoted as M (M = Fe(II), Co(II), Cu(II), Mn(II), Mn(III), Zn(II), Ni(II), and so on), are doped on the mother IONPs, with a spinal structure have been successfully employed as a biocatalyst.[70,71]As a result of their crystalline solid structure, exacerbated magnetism, large active surface area, and superparamagnetic performance, they were considered promising biocatalysts.[72,73]Previous investigation has demonstrated that doping mechanisms can be developed by exchanging a TMIs with a second transition metal ions (TMIS).[74] As a consequence, an individual Fe atom had to be replaced by TMIS, such as Ce(IV), Co(II), and Mn(II), to form the exterior surface of doped-IONPs.[75] The optimized metal doping configurations are shown in the illustration (Figure 1). As a result, an individual Fe atom had to be replaced by a TMIS such as Ce(IV), Co(II), and Mn(II). After optimization, the corresponding distance (bond length) between M and O atoms is 2.198, 1.889, and 1.962 for Ce, Co, and Mn, respectively, while this was 1.9777 for Fe−O (before doping).[76] This is mainly due to the different ionic radii of this metal. The Bader charge calculation was employed

https://doi.org/10.1021/acsomega.3c06323
ACS Omega 2024, 9, 16−32

Table 1. Antimicrobial Activity and Potential Mechanism(s) of Action of Doped-IONPs[a]

Doped materials	Nanoparticles	Size (nm)	Synthesis methods	Coating materials	Organisms	Conc. of nanoparticles (μg/mL)	ZOI (mm)	MIC (μg/mL)	MBC (μg/mL)	Mechanisms	Ref.
Ni	Ni-doped Fe_2O_4	15−200	CPA	NDG	*E. coli*	50	16	50	NR	The bacterial membrane is disrupted by Ni^{2+} and Fe^{3+}ions interactions with membrane proteins, which additionally hinders the growth of bacteria.	24
				Cellulose	*B. subtilis*	50	14	50	NR		
	Ni-doped Fe_3O_4/ZnO	28−33	MAP	ZnO	*K. pneumoniae*	NR	13	NR	NR	The microwave and sonication of Fe_3O_4/ZnO nanocomposites and different NDIZ had a significant impact on ROS-assisted toxicity. The ultrasonication process allows Ni ions to reach the Fe_3O_4/ZnO surface and generate greater ROS in the solution. It triggered oxidative stress in the bacteria, which results in cell disintegration.	25
					S. aureus	NR	17	NR	NR		
	Ni-doped-Fe_3O_4/ZnO	36	MAP	ZnO	*K. pneumoniae*	NR	6	NR	NR		
					S. aureus	NR	6	NR	NR		
Cu	Cu-doped α-Fe_2O_3	20−60	GC	PEI	*P. vulgaris*	400	16 ± 1.0	250	NR	Particles disrupt cell wall, inducing oxidative stress and cell lysis. It promotes oxidation of proteins and DNA by producing ROS.	26
					Serratia marcescens	400	16.67 ± 0.58	250	NR		
					Streptococcus mutants	400	10	250	NR		
					B. cereus	400	15 ± 1.0	NR	NR		
	Cu-doped-α-Fe_2O_3	21	CP	NR	*E. coli*	400	20	600	NR	ROS formation, which causes oxidative stress. Free radicals lead to bacterial death by breaking down the DNA strands, peroxidation of membrane lipids, inactivation of enzymes and depolymerization of polysaccharides.	27
						600	23 ± 1				
						800	25				
					B. subtilis	400	16	600	NR		
						600	19				
						800	23				
					S. aureus	400	18	750	NR		
						600	18				
						800	20				
					Salmonella typhi	400	15 ± 1.0	600	NR		
						600	20 ± 1.0				
						800	23				
Co	Co-doped Fe_3O_4	10−14	CP	NR	*Shigella dysenteriae*	1−2048	NR	>2048	>2048	The nanoparticles adhere to the plasma membrane, disrupting it and ensuring that the ROS penetrates simultaneously to the lipids. But the electron emitted from the iron atom in the presence of cobalt(III) might be retained by the Co (III) and converted to the highly stable Co (II) and causing no formation of highly oxidized species and less activity.	28
					K. pneumoniae	1−2048	NR	>2048	>2048		
					Acenetobacter baumnii	1−2048	NR	>2048	>2048		
					Streptococcus pyogene	1−2048	NR	>2048	>2048		
Zn	ZnO-doped-Fe_3O_4	75.90	CP	NR	*E. coli*	250000	14	NR	NR	Negatively charged organisms and positively charged metal nanoparticles get attracted to one another. Consequently, the bacteria are oxidized and exterminated. Metal ions and thiol groups on the outermost layer of bacteria interact primarily as a result of cell breakage. Another route for bacterial protein and DNA damage might be ROS, including OH, O_2, and H_2O_2.	36
					S. aureus	250000	10	NR	NR		
	ZnO-doped-Fe_3O_4	34.99	CP	Ag	*E. coli*	250000	19	NR	NR	ZnO-based nanocomposites aggregate at cell membrane or cytoplasm of bacterial cells. Zn^{2+} ions are released as a result, which promotes the death of bacteria and membrane damage.	36
					S. aureus	250000	11	NR	NR		
	ZDI: Zn-doped-Fe_2O_3	10−40	STM	NR	*Microcystis aeruginosa*	50000	NR	NR	NR	Magnetic Zn-doped Fe_3O_4 particles have a photocatalytic inactivation effect—the photocatalytic pretreatment produced superoxide radicals responsible for mucilage desorption. Therefore, the influence of mucilage desorption on microorganisms during the photocatalytic process may be used to explain the increased cell elimination.	116

https://doi.org/10.1021/acsomega.3c06323
ACS Omega 2024, 9, 16−32

Table 1. continued

Doped materials	Nanoparticles	Size (nm)	Synthesis methods	Coating materials	Organisms	Conc. of nanoparticles (μg/mL)	ZOI (mm)	MIC (μg/mL)	MBC (μg/mL)	Mechanisms	Ref.
	ZDI: Zn-doped-Fe_2O_3	28	SGP	NR	*K. pneumoniae*	25	16	75	NR	Generate ROS-induced bacterial harm. Subsequently, intracellular cytoplasmic leakage of both sugar and protein suggests their capacity to compromise bacterial membrane integrity.	50
						50					
						75					
	ZDI: Zn-doped-Fe_2O_3	47.9 ± 2.5	CP	NR	*E. coli*	12.5	9 ± 0.8	NR	NR	The bactericidal effectiveness of nanoparticles is mediated by bacterial cell death induced by membrane rupture, protein leakage, and ROS production.	30
						25	10 ± 0.4				
						50	10 ± 0.6				
						100	11 ± 0.7				
					P. aeruginosa	12.5	10 ± 0.8				
						25	11 ± 0.4				
						50	11 ± 0.5				
						100	12 ± 0.8				
					K. pneumoniae	12.5	10 ± 0.5				
						25	10 ± 1				
						50	11 ± 1.1				
						100	13 ± 1.6				
					S. typhi	12.5	8 ± 0.5				
						25	10 ± 0.7				
						50	11 ± 1.4				
						100	12 ± 1.1				
					S. aureus	12.5	10 ± 0.5				
						25	10 ± 0.6				
						50	11 ± 0.8				
						100	13 ± 0.9				
Se	Se-doped-Fe_3O_4	80	CP	NR	*S. aureus*	10000	18	NR	NR	Combination of Se nanoparticleseffectively increases the formation of ROS. The most generally recognized mechanism of action for selenium nanoparticlesis particle attachment to the bacterial membrane and selenium ion discharge into the bacterial cell, resulting in oxidative stress, protein synthesis inhibition, or DNA mutation.	31
					Staphylococcus saprophyticus	10000	2	NR	NR		
					P. aeruginosa	10000	8	NR	NR		
					K. pneumoniae	10000	6	NR	NR		
					E. coli	10000	11				
Cr	Cr-doped-$CeFe_2O_4$	1.64	CP	NR	*S. aureus* (ATCC 25993)	800	NR	10	200	The major mechanism could be ROS-related oxidative stress, such as superoxide radicals, hydroxyl radicals, and hydrogen peroxide (H_2O_2), damaging bacterial DNA and proteins. In this instance, magnetite may be regarded as the source of the ROS that reduced the growth rate of *S. aureus*. Additionally, the use of transition metals—especially chromium—can have a negative impact on the topology and the replication and transcription of bacteria.	52
								50	400		
Ca	Ca-doped-Fe_3O_4	5−10	CP	CLP	*E. coli*	5000	NR	NR	NR	Dose-dependent toxicity of nanoparticles leads to bacterial cell rupture.	51
					S. aureus	5000	NR	NR			
					Salmonella enteritidis	5000	NR	NR			
					P. aeruginosa	5000	NR	NR			
Mo	Mo-doped-Fe_3O_4	36.11	CP	NR	*E. coli*	20000	3.45	NR	NR	By ROS formation, positive radicals rapidly enter bacterial cell membranes, causing bacterial death. Compared to negatively charged radicals, which can damage the surface of bacterial cells but cannot penetrate through the outer membranes of bacteria, such hydroxyl radicals along with superoxide anions.	32
		38.45									
		25.74									
		24.38				400000	1.45	NR	NR		

https://doi.org/10.1021/acsomega.3c06323
ACS Omega 2024, 9, 16−32

Table 1. continued

Doped materials	Nanoparticles	Size (nm)	Synthesis methods	Coating materials	Organisms	Conc. of nanoparticles (µg/mL)	ZOI (mm)	MIC (µg/mL)	MBC (µg/mL)	Mechanisms	Ref.
Au	Au-doped-Fe_3O_4	11.9 ± 0.15	HDA	DL-methionine	*A. baumannii*	70000	NR	NR	NR	Strong ionic contact of nanoparticles with bacterial cell membranes increases the permeability, leading to cell death.	34
					S. enterica	70000	NR	NR	NR		
					S. aureus	70000	NR	NR	NR		
					Micrococcus luteus	70000	NR	NR	NR		

[a]Ref.: References; Conc.: Concentrations; ZOI: Zone of inhibition; MIC: Minimum inhibitory concentration; MBC: Minimum bactericidal concentration; NR: Not reported; ROS: Reactive oxygen species; OH: Hydroxyl radicals; O_2: Superoxide anion radicals; H_2O_2: Hydrogen peroxide; PEI: Polyethylenimine; MAP: Microwave-assisted process; CP: Coprecipitation; GC: Green combustion; CPA: Chemical polymerization approach; SGP: Sol−gel process; HDA: Hydrothermal approach; STM: Solvothermal method; NDG: Nitrogen-doped graphene; CLP: Calcium phosphate.

to investigate these doping possessions further to estimate the standard deviation of the active charge of Fe(II), Co(II), Ce(IV), and Mn(II) metals.

The average active charge (Q) has been determined by $Q = Z_{val} - Q_{bader}$, whereas Q_{bader} and Z_{val} symbolize an atom's Bader charge and number of valence electron, respectively, and if Z_{val} has a positive number, it indicates the process of metal electron loss. For example, Xie et al. (2021)[76] performed a comprehensive study to compare the Z_{val} value for various TMIs doped with iron oxide nanoparticles, where all metal ions have demonstrated a positive Z_{val} value though losing electrons. For the Fe(II), Ce(IV), Co(II), and Mn(II) atoms, the values were 8.0, 12.0, 9.0, and 7.0, respectively, which indicates that these metals lost their electrons during the doping process. In contrast, the Ce atom exhibits a significant level of electron variations on the γ-Fe_2O_3 lattice and has a greater tendency to donate electrons to atoms around it. As illustrated in Figure 1b−d, the electron density of the γ-Fe_2O_3 (001) lattice with these TMIs reveals doped atoms with a substantial molecular interaction among the doped metal ions and the γ-Fe_2O_3 lattice. From the comparison of the outermost orbits of free these TMIs with the same atoms on the doped γ-Fe_2O_3 composite's surface, it was found that doped Fe(II), Mn(II), Co(II), and Ce(IV) atoms have more hybridized **d**-orbitals than free atoms.[76] After doping, there is apparent hybridization in both the **d** and **f** orbitals of the Ce atom, suggesting that there is a strong electrostatic interactions between both orbitals with the surroundings of O atom, as established by Jarlborg et al. (2014).[77]

3.2. Different Biomedical Applications of Doped-IONPs. Doped-IONPs have diverse applications in various fields of biomedicine—for instance, in MRI,[78,79] visualization and diagnostics,[80] cancer therapy with magnetic hyperthermia,[81] photodynamic therapy,[82] development of biosensors,[83] environmental remedies,[31] and tissue engineering[84,85] (Figure 2). Recently, experimental biomedical imaging field has gotten more focused on the fabrication of novel contrast agents with multimodal and versatile features of doped-IONPs.[86,87] In a standard MRI system, doped-IONPs can be employed at low concentrations as suitable negative contrast agents.[82,88−90]Additionally, doped-IONPs are ideal for cell labeling as perspective contrast agents. The optimum concentration of doped-IONPs within a nontoxic concentration range was 0.154 mM reported by Mohammadi et al. (2020).[88] These doped-IONPs demonstrate high T2 relaxivity, biodistribution, and long circulation time.[88,90] IONPs doped with transition metal are also employed to minimize the size of superparamagnetic contrast agents while retaining an excellent MRI contrast efficiency.[91]

A recent study by Nowicka et al. (2023)[92] reported magnetic IONPs doped with magnesium have demonstrated outstanding potential for magnetic fluid hyperthermia (MFH) in lung cancer treatments. MFH is a potential treatment technique that uses magnetic doped-IONPs exposed to an alternating magnetic field to heat malignant tissues to 40−43 °C.[92] Doped-IONPs also exhibited controlled drug delivery, enhanced targeted delivery, improved stability and biocompatibility.[93,94] In addition to that doped-IONPs are becoming essential for photodynamic therapy carrier due to its ability to penetrate deeply.[95] Moreover, environmental remedies, *e.g.*, water treatment, can be performed by utilizing the absorbance ability of doped-IONPs.[31] Tissue engineering is also conceivable via doped-IONPs as the magnetic field aids in

https://doi.org/10.1021/acsomega.3c06323
ACS Omega 2024, 9, 16−32

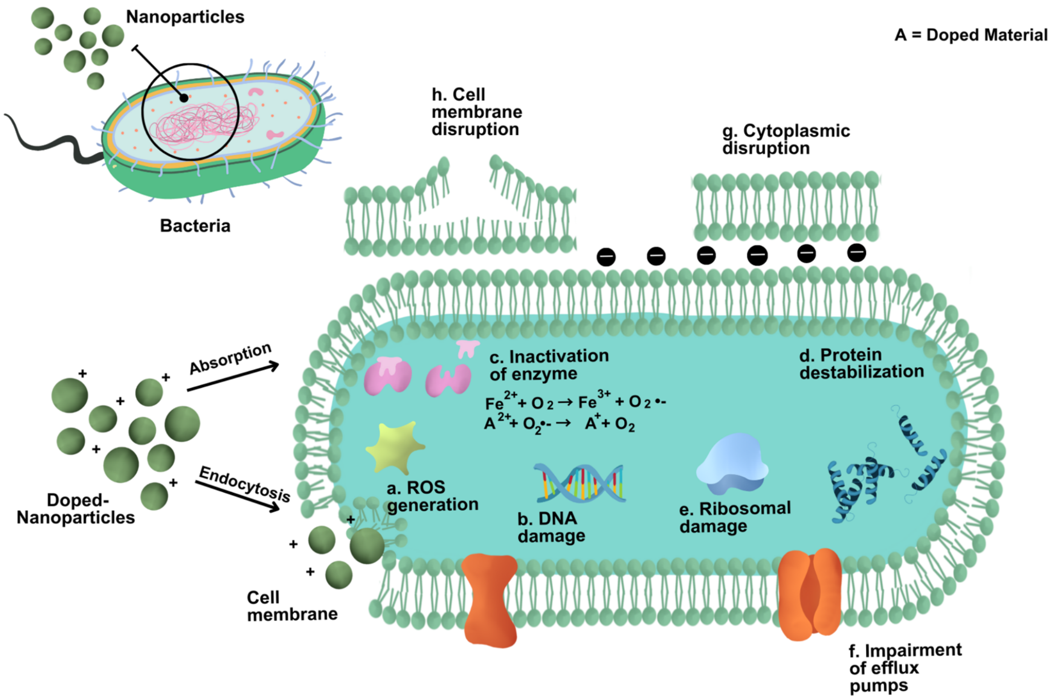

Figure 4. Mechanism of actions of doped-IONPs antimicrobial activity. Particles trigger oxidative stress and cell lysis by (a) generating ROS, (b) damaging DNA, (c) inactivating enzymes, (d) destabilizing proteins, (e) damaging ribosome, (f) impairing efflux pump, (g) disrupting cytoplasm, and (h) cell membrane. ROS: Reactive oxygen species; Doped-IONPs: Doped-iron oxide nanoparticles; IONPs: Iron oxide nanoparticles.

cellular mechanotransduction toward guided differentiation.[84,85] Acceptable selectivity, stability, and sensitivity have also made doped-IONPs a perfect candidate for biosensor.[96]

3.3. Antimicrobial Activities of Doped-IONPs. Bare nanoparticles possess inherent properties which can be further enhanced by doping foreign metals.[97] One of the notable modifications is the enhancement of antimicrobial activity through different doping methods.[97] Doped-IONPs sized around 20−200 nm have shown significant antimicrobial activity on different bacteria, where size less than 20 nm.[28,29,52] While doped-IONPs larger than 200 nm demonstrated comparatively poor antimicrobial activity.[24−26,29,30,36] Additionally, IONPs doped with transition metals shown significant antimicrobial activity based on the synthesis process, size, concentrations, and application.[25,30,50] Doped-IONPs were synthesized by using CP, CPA, MAP, GC, SGP, HDA, and solvothermal approach. However, the CP method was the most approached one due to its less complexity.[24,25,27,30,36] Moreover, the core advantage of the CP method over other synthesis methods is generating a large scale of nanoparticles. The CP method can successfully modify the particles size and shape by altering ionic strength, pH, temperature, the type of the salts, *e.g.*, chlorides, perchlorates, nitrates, and sulfates, or the concentration ratio of Fe−II/Fe-III.[98] According to the thermodynamics of the CP method, IONPs precipitation should be expected in a nonoxidizing oxygen environment with a pH range of 8 to 14 and in a stoichiometric ratio of 2:1 (Fe^{3+}/Fe^{2+}).[99] In this method, the size of the particles can be adjusted by adding or changing different stabilizers and iron oxide ratios.[100]

The influence of nanoparticles on bacteria varies by strain/species.[101,102] One of the major reasons why pathogens are prone to nanoparticles could be their compositions of cell walls and cell membranes.[103,104] Moreover, Gram-positive bacteria might be more sensitive toward IONPs due to their lack of cell membrane and cell wall polarity.[105,106] The cell wall of Gram-negative bacteria, in contrast, is more structurally and chemically complicated, with a cell membrane made of phospholipids proteins, lipopolysaccharides, and a thin layer of peptidoglycan.[107] Furthermore, Gram-negative bacteria consists of lipopolysaccharides in the outer cell membrane which elevate the net negative charge, consequently repelling negatively charged free radical penetration.[102] As a result, Gram-negative bacteria are claimed to be less vulnerable to IONPs.[106] Additionally, Gram-positive bacteria rely only on the peptidoglycan layer making it more vulnerable to lower concentrations.[105,106,108] Hence, the use of bare or metal-doped nanoparticles, especially doped-IONPs, as antimicrobial agents is justified.[24,25,109−113]

A study by Morais et al. (2021)[114] showed that $ZnFe_2O_4$, $CoFe_2O_4$, and $Zn_{0.5}Co_{0.5}Fe_2O_4$ exhibited antimicrobial activity against Gram-positive (*Staphylococcus aureus*) and Gram-negative bacteria (*E. coli*) where Gram-positive bacteria were more vulnerable to doped-IONPs than Gram-negative bacteria (Figure 3).[114] Additionally, the ZOI produced for $ZnFe_2O_4$ nanoparticles was slightly larger than that for low-temperature calcined nanoparticles. This means that low-temperature calcined nanoparticles crystalline structure was moderately more efficient in inhibiting both strains.[114] At lower temperatures, small particles were formed and the possible reason smaller particles were more destructive than the larger one could be smaller particles are efficient in cell uptake than larger particles (Figure 3).[115] The highest ZOI was created in the order of $ZnFe_2O_4$ > $Zn_{0.5}Co_{0.5}Fe_2O_4$ > $CoFe_2O_4$ indicating that the produced ferrites have dose-inhibitory capacity dependence.[114]

Metal-doped with IONPs, e.g., Zn-doped-IONPs (ZDI), Cu-doped-IONPs (CDI), Ni-doped-IONPs (NDI), Se-doped-

https://doi.org/10.1021/acsomega.3c06323
ACS Omega 2024, 9, 16−32

Table 2. Antimicrobial Activities of Metal-Doped Magnetic Nanoparticles[a]

Doped materials	Nanoparticles	Size (nm)	Synthesis methods	Stimuli	Coating materials	Organisms	Conc. of NPs (μg/mL)	ZOI (mm)	MIC (μg/mL)	MBC (μg/mL)	Mechanisms	Ref.
Ni	Ni-doped MgO	14.15–12.43	SGP	NR	NR	*E. coli*	40	7.8 ± 0.289–9.3 ± 0.289	40	NR	Ni, Co, Fe doping could decrease the size of the nanoparticles aiding the penetration of the particles into the bacterial cell. Nanoparticles could also generate ROS and damage DNA. Moreover, Ni, Co and Fe interacted with the thiol groups of the essential enzyme present in the bacteria, leading to death.	139
							80	8.8 ± 0.289–11.3 ± 0.289				
						S. aureus	40	6.3 ± 0.289–8.0 ± 0.00				
							80	7.5 ± 0.00–9.3 ± 0.289				
Co	Co-doped MgO	14.51–11.49		NR	NR	*E. coli*	40	8.0 ± 0.00–10.3 ± 0.289	40	NR		
							80	9.0 ± 0.00–12.3 ± 0.289				
						S. aureus	40	6.8 ± 0.289–8.5 ± 0.00				
							80	7.7 ± 0.289–9.5 ± 0.00				
Fe	Fe-doped MgO	13.88–10.57		NR	NR	*E. coli*	40	8.2 ± 0.289–11.8 ± 0.289	40	NR		
							80	10.8 ± 0.289–14.7 ± 0.289				
						S. aureus	40	7.0 ± 0.00–9.5 ± 0.00				
							80	9.0 ± 0.50–11.7 ± 0.00				
Co	Co-doped Ag	2.5 ± 0.2	LAL	Magnetic field	NR	*E. cloacae*	20	NR	NR	NR	By utilizing Ag nanoparticles in combination with Co or Fe, the overall antibacterial impact could be improved as an effective bactericidal agent, which could be later engineered to respond to external magnetic fields to destroy the biofilm and ROS generation. The interaction with a growing number of bacteria was made possible by the magnetically propelled movement of the magnetic nanoparticles through the biofilm.	140
						E. faecalis						
						P. putida						
						B. subtilis						
Fe	Fe-doped Ag	2.9 ± 0.1	LAL		NR	*E. faecalis*	20	NR	NR	NR		
						E. cloacae						
						B. subtilis						
Cu	Cu-doped ZnO	60–70	STM	Light	NR	*E. coli*	NR	NR	NR	NR	Nanoparticles might penetrate themselves to the cell walls of bacteria, causing devastation, ROS generation and ultimately death of the cells. Cu-doped ZnO might cause more destruction due to higher levels of Cu^{+} release. Moreover, doping could boost the potency of photocatalytic degradation by decreasing band gap energy.	141
						S. aureus	NR	NR	NR	NR		
Ag	Ag-doped FSZ	NR	STM	Dark	NR	*E. coli* (ATCC 1105)	~5000	26.4	100000	NR	Ag and Zn doping might increase the antimicrobial activity through rapid release of ions. Moreover, exposing nanoparticles in light could generate and excite more ROS, leading to bacterial cell death.	142
						S. aureus (BBRC 10050)		25.6	100000	NR		
Cu	$Zn_{1-x}Cu_xO$	29	HDA	Light, pH, catalyst doze	NR	*S. aureus*	x = 0.0%	5 ± 0.3	NR	NR	Due to light exposure, nanoparticles produced ROS which might attack the microorganism and degrade the cell. Moreover, the surface charge of the particles could be controlled by pH. Decrease of pH could increase the surface charge of nanoparticles resulting in attacking more bacteria	143
							x = 1.5%	7 ± 0.2				
							x = 3.0%	8 ± 0.2				
							x = 4.5%	10 ± 0.2				
						B. subtilis	x = 0.0%	5 ± 0.1	NR	NR		
							x = 1.5%	7.5 ± 0.3				

https://doi.org/10.1021/acsomega.3c06323
ACS Omega 2024, 9, 16−32

Table 2. continued

Doped materials	Nanoparticles	Size (nm)	Synthesis methods	Stimuli	Coating materials	Organisms	Conc. of NPs (μg/mL)	ZOI (mm)	MIC (μg/mL)	MBC (μg/mL)	Mechanisms	Ref.
							x = 3.0%	9 ± 0.2				
							x = 4.5%	11 ± 0.2				
						E. coli	x = 0.0%	5 ± 0.2	NR	NR		
							x = 1.5%	10 ± 0.3				
							x = 3.0%	12 ± 0.2				
							x = 4.5%	15 ± 0.5				
						P. maltocida	x = 0.0%	5 ± 0.3	NR	NR		
							x = 1.5%	10.5 ± 0.2				
							x = 3.0%	12 ± 0.5				
							x = 4.5%	16 ± 0.3				
Zr	Zr-doped TiO_2	13.5–21.59	SGP	Solar light, methylene blue	NR	*E. coli*	10	16 ± 3.6–25 ± 2.64	NR	NR	ROS produced when oxygen and dehydrogenase enzymes interacted with Zr-doped TiO_2 nanoparticles in organism, increasing the antibacterial activity.	144
							15	14 ± 1.74–20 ± 1.52				
							20	20 ± 3.00–23 ± 2.65				
							25	16 ± 3.60–25 ± 3.61				
						P. aeruginosa	10	18 ± 1.00–23 ± 1.45	NR	NR		
							15	16 ± 2.64–20 ± 1.33				
							20	16 ± 3.61–18 ± 1.41				
							25	16 ± 2.0–25 ± 3.61				

[a]Ag-doped FSZ: Ag-doped γ-Fe_2O_3@SiO_2@Zeolitic imidazolate framework-8; ROS: Reactive oxygen species; NR; Not reported; HDA: Hydrothermal approach; LAL: Laser ablation in liquid; SGP: Sol–gel process; STM: Solvothermal method.

https://doi.org/10.1021/acsomega.3c06323
ACS Omega 2024, 9, 16–32

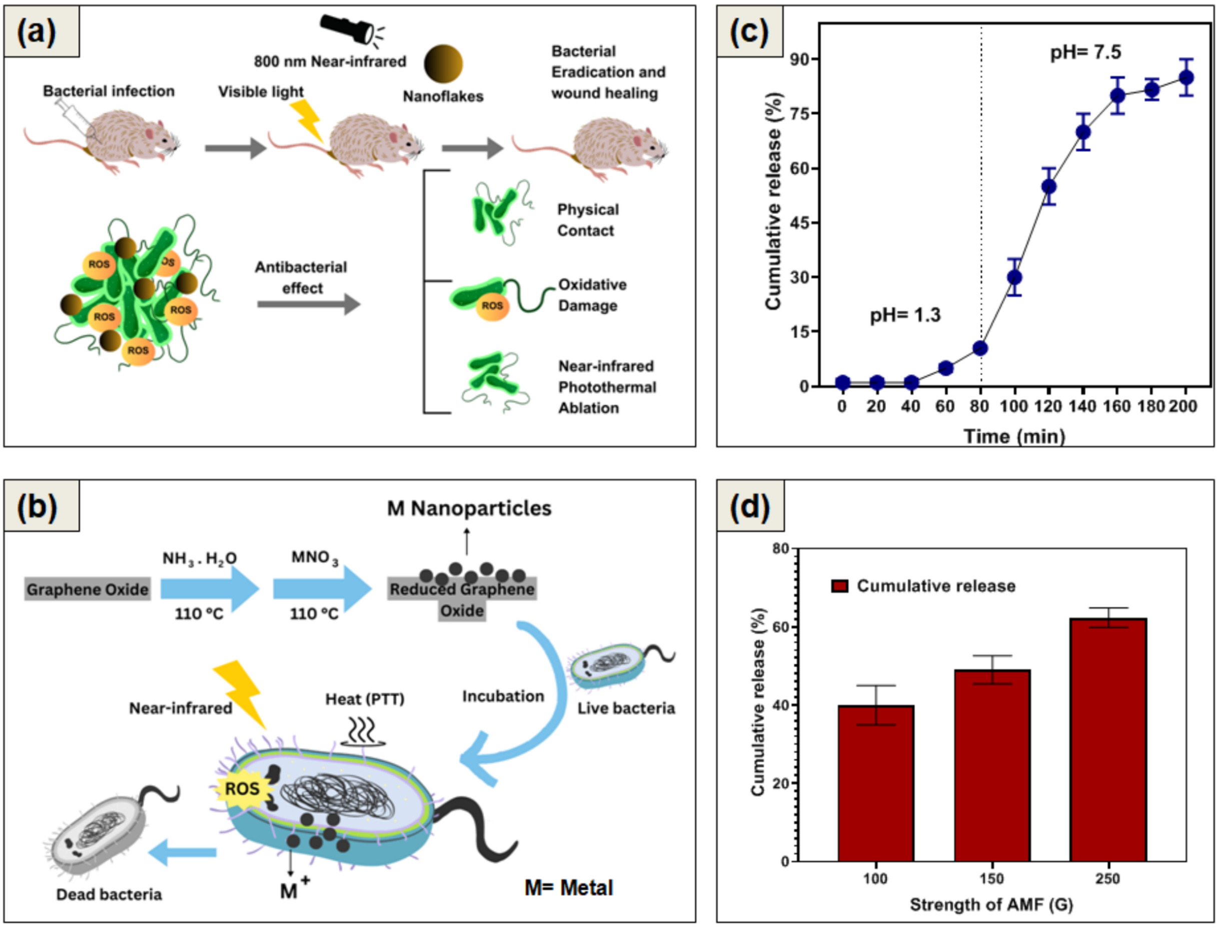

Figure 5. Schematic illustration of the effects of nanoparticles triggered by different stimuli. (a) Antibacterial therapy of photoactivated nanoflakes induced by photocatalytic and photothermal activity. Antibacterial activity is mediated by a synergistic combination of electrostatic contact, ROS driven oxidative damage, and photothermal inactivation, which clearly damage the cell membranes of bacteria. (b) When exposed to near-infrared radiation, reduced graphene oxide photothermal effect was much stronger to increase M^+ release (derived from nanoparticles) which generates ROS stress, eventually breaking the integrity of bacterial cells. (c) Higher drug release due to increased pH, leading to higher antibacterial activity. (d) Drug cumulative release increased by external magnetic field. Alternating the magnetic field increases the agitation and motion of magnetic nanoparticles, leading to enhanced antibacterial activity. These images indicate potential results but do not reflect any actual experiments.

IONPs (SDI), Au-doped-IONPs, Cr-doped-IONPs, and Ca-doped-IONPs (KDI) have shown higher antimicrobial activity against resistantbacteria (*Bacillus subtilis*, *Klebsiella pneumoniae*, *E. coli*, *S. aureus*, *Proteus vulgaris*) compared to Mo-doped-IONPs (MDI), Co-doped-IONPs (CBDI), in terms of zone of inhibition (ZOI) (Table 1). Among all the metal doped-IONPs, ZDI, CDI, and SDI have shown the highest bacterial inhibition based on ZOI (≥20 nm).[26,31,36] In contrast, KDI, MDI, and CBDI have shown the lowest ZOI against different bacteria (except on *S. aureus*).[25,28,32,51] Doping activity of ZDI at the lowest concentration was comparatively higher than any other doped-IONPs.[30] Apart from ZOI, minimum inhibitory concentration (MIC) was performed to determine the lowest concentration which can inhibit the growth.[24−26,28,30,32] Studies of NDI and ZDI have shown higher MIC with the lowest amount on *E. coli*, *B. subtilis*, *S. typhi*, *K. pneumonia*, while MDI has shown no significant inhibition of *E. coli* at the highest concentration (Table 1).[32] MIC and minimum bactericidal concentration were not reported in most studies.[25,29−32,34,36,51,116]Although research by Ivashchenko et al. (2015) reported a higher antimicrobial activity of doped-IONPs combined with antibiotics.[117] The author also mentioned in a different study that doped-IONPs combined with antibiotics discharged iron ions almost twice as much as bare IONPs at a pH of 5 in response to the formation of the galvanic couple with metal, leading to a higher antimicrobial activity.[118] Doped-IONPs and bare IONPs shared similar mechanism of actions from generating ROS for disrupting the bacterial DNA and membrane, leading to cell death eventually.[25,28−32,34,36,51,52,116]

4. MECHANISMS OF THE DOPED-IONPS ANTIMICROBIAL ACTIVITY

Although it has been demonstrated that doped-IONPs exhibit antimicrobial activity against a variety of pathogens, including Gram-positive, Gram-negative bacteria and fungi, little has been revealed about the precise mechanism behind such antimicrobial action. Nonetheless, a substantial study has been conducted to understand their method of action, and four well-defined mechanisms have been postulated thus far: (i) oxidative stress by ROS generation, (ii) reduced expression of antibiotic resistance genes, protein, and enzyme deactivation, (iii) disruption of the cell wall and DNA replication, and (iv) impairment of efflux pump (Figure 4).

https://doi.org/10.1021/acsomega.3c06323
ACS Omega 2024, 9, 16−32

4.1. ROS Generation. Doped-IONPs exhibit mechanisms of antimicrobial activity similar to those of bare IONPs. One of the typical mechanism is ROS[119,120]generation, which can occur during photocatalysis, Fenton reactions, etc.[121] ROS damage the DNA molecules by its genotoxic action.[120,122] The production of ROS leads to oxidative stress.[122] Bacterial mortality is caused by free radicals in various ways, including the depolymerization of polysaccharides, peroxidation of membrane lipids, breaking of DNA strands, and inactivation of enzymes.[27] An activity reduction in the antioxidant systems enzymes such as catalase and glutathione reductase can be generated by increased ROS concentration.[123] Additionally, doped-IONPs can destroy the integrity of bacterial cell membranes.[36,51]The combination of the foreign metal with nanoparticles by the doping method can effectively increase the formation of ROS.[124] Besides that, with the addition of doped particles, the spherical morphology of nanoparticles can shift to a nanofoil-like structure, which enhances antimicrobial activity.[125]

At the interface of metal doped-IONPs, electron trapping may occur.[126] The reduction of Fe^{3+} ions to Fe^{2+} ions utilize the electrons from the Fermi energy level (the highest energy level an electron occupies at the absolute zero temperature) of metal oxide and as a result, decreases the recombination of electron−hole. Such electron-trapping methods increase the ternary nanocomposite photocatalytic effectiveness.[36] Since Fe^{2+} ions are less stable, they are rapidly oxidized by oxygen molecules.[126−128]The electrons released throughout this oxidation reaction generate superoxide ions ($O_2^{\bullet-}$), and the holes that are produced at the IONPs surface form the hydroxyl radical ($OH^{\bullet}$).[11] The basic ROS[36] reaction process involves

$$Fe^{3+} + e^- \rightarrow Fe^{2+}$$
$$Fe^{2+} + O_2 \rightarrow Fe^{3+} + O_2^{\bullet-}$$
$$M^{2+} + O_2^{\bullet-} \rightarrow M^+ + O_2$$
$$Fe^{2+} + H_2O_2 \rightarrow Fe^{3+} + {}^{\bullet}OH + OH^-$$
$$O_2^{\bullet-} + H_2O_2 \rightarrow OH^- + {}^{\bullet}OH$$

where "M" represents transition metal(s).

4.2. Reduced Expression of Antibiotic Resistance Genes, Protein,and Enzyme Deactivation. Similar to IONPs, doped-IONPs can also bind to functional groups of proteins, *e.g.*, mercapto (−SH), carboxyl (−COOH), and amino (−NH), particularly those in enzymes, causing deregulation or partial inhibition and a reduced expression of genes linked to antibiotic resistance in bacteria.[119,129,130]

4.3. Disruption of Cell Wall and DNA Replication. Using transition metals by doping method, particularly chromium can affect the topology and affect bacteria's DNA replication and transcription.[130,131]Doped-IONPs can enter the cytoplasm,[132] accumulate there, and damage cell wall in the same way as bare IONPs.[20,133]Moreover, F0/F1-ATPase activity, the rate of H(+) channel via the cell membrane and affect the redox potential.[134] Multiple experiments have been performed to evaluate the antimicrobial activity of doped-IONPs due to their size and resemblance to other types of metal IONPs.[36]

4.4. Impairment of Efflux Pump. There are two potential ways in which metal-doped-IONPs can prevent efflux pumps from functioning. In order to prevent the release of antibiotics outside of the cells, one potential strategy is the immediate attachment of doped-IONPs to the active site of efflux pumps. The binding location of efflux pumps may be affected by metal-doped nanoparticles acting as a competitive antibiotic inhibitor in this instance.[135] Disrupting efflux kinetics is another potential mechanism.[136] Metal nanoparticles may result in the termination of the proton gradient, which results in the membrane potential being disrupted or the loss of the proton motive force, weakening the driving force required for the efflux pump to function.[135,137,138]

5. METAL-DOPED MAGNETIC NANOPARTICLES FOR ANTIMICROBIAL APPLICATIONS AND EFFECT OF DIFFERENT STIMULI

Like metal-doped IONPs, metal ion-doped other magnetic nanoparticles have also demonstrated potential for their application as antimicrobial agent, *e.g.*, Ni, Co, and Fe-doped MgO,[139] Co, Fe-doped Ag,[140] Cu-doped ZnO,[141] Ag-doped γ-Fe_2O_3@SiO_2@Zeolitic imidazolate framework-8 (Ag-doped FSZ),[142] $Zn_{1-x}Cu_xO$,[143] Zr-doped TiO_2[144] magnetic nanoparticles. Among all the metal ion doped magnetic nanoparticles listed here, Ag-doped FSZ exhibited the highest ZOI (26.4 mm) against *E. coli* (ATCC 1105) under the dark environment, while lowest ZOI (5 ± 0.1 mm) against *B. subtilis* was observed after $Zn_{1-x}Cu_xO$ treatment (Table 2).[142,143] Moreover, Ag-doped FSZ and Ni, Co, and Fe-doped MgO showed the highest (100000 μg/mL) and lowest (40 μg/mL) MIC against *E. coli* and *S. aureus*, respectively.[139,142] It should be noted that MIC values for other metal ion-doped magnetic nanoparticles were not reported.[140,141,143,144] These metal-doped magnetic nanoparticles (Ni-, Co-, and Fe-doped MgO[139]) interacts with the thiol groups found in essential bacterial enzymes, leading to their inactivation and cell death.[145] Moreover, metal doping could also influence the size and magnetic properties of the magnetic nanoparticles by decreasing the energy band gap[146] and combining electronic charges with spins.[147,148]As the size of metal-doped nanoparticles decreased, the antimicrobial activity could increase due to higher surface to volume ratio, facilitating greater interaction with bacterial cell.[143] Additionally, doping metals (Co, Fe,[140] Cu,[141,143] Zn[143]) could also increase the charge density on the nanoparticles surface, contributing to higher ROS generations.[149] Magnetic behaviors of the nanoparticles (Co, Fe-doped Ag[140]) mechanically damage the microorganisms, increasing the antimicrobial activity of the magnetic metal-doped nanoparticles.[150]

On rare occasions, the antimicrobial properties of doped nanoparticles could be triggered by different stimuli, *e.g.*, light,[141−144] temperature,[114] pH,[143] magnetic field,[140] and catalyst concentration[143,144] (Figure 5). Shujah et al. (2022)[32] reported that when MDI was exposed to light irradiation with photon energy, excited electrons get trapped by the molecular oxygen (O_2) present on the surface, resulting in production of greater superoxide anion radicals.[151,152] Moreover, increase of pH could also elevate the negative charge resulting in adsorbing more OH^- ions, promoting the formation of higher ${}^{\bullet}OH$ free radicals.[153] Likewise, upon exposure to solar light Zr-doped TiO_2 nanoparticles demonstrated higher ZOI around 16 ± 3.6 mm to 25 ± 3.61 mm against *E. coli* and *P. aeruginosa* compared to unexposed particles.[144]

6. CONCLUSIONS AND FUTURE DIRECTIONS

Doped-IONPs have substantially presented antimicrobial activities that are higher than those of bare IONPs. The antimicrobial activity of doped-IONPs varies depending on

https://doi.org/10.1021/acsomega.3c06323
ACS Omega 2024, 9, 16−32

factors, *e.g.*, particle size, coating materials, and synthesis methods. Doped-IONPs ranging from approximately 20−200 nm have shown notable antimicrobial activity on different bacteria. In other words, nanoparticles smaller than 20 nm and larger than 200 nm demonstrated lower levels of antimicrobial activity. Although different-sized metal-substituted doped-IONPs at different calcination temperatures display dose-dependent inhibition due to their high metal molarities and small size. Lower calcination temperature produces smaller particles. In addition, higher metal molarities and a smaller size exhibit greater cell uptake and destruction. Moreover, among all the synthesis methods, the CP method emerged as the most convenient approach due to its ability to enable surface modification, large-scale manufacturing, and precise temperature and pH control during the synthesis process. However, the biocompatibility of IONPs relies on the choice of doping material.[70,71] Doping nontoxic metals, *e.g.*, Ag,[154] Au,[155] Zn,[156] Al[157] on IONPs has shown reduced or no toxicity. Conversely, toxic heavy metals and metal oxides, *e.g.*, Cr,[158] TiO_2,[159] could increase the toxicity of IONPs.

One of the main challenges of using doped-IONPs is their toxicity and propensity to aggregate due to strong magnetic attraction and enormous surface energy.[160] To address these issues, different surface modification materials can be utilized for the coating of doped-IONPs such as polymers (*e.g.*, polyethylene glycol,[161] monomers (*e.g.*, citrate[161]), silica,[162] chitosan[163,164] to increase the stability. During the past ten years, plant-mediated synthesis has also become a viable alternative to conventional methods for synthesizing.[40]

AUTHOR INFORMATION

Corresponding Author

Md Salman Shakil − *Department of Mathematics and Natural Sciences, Brac University, Dhaka 1212, Bangladesh;* orcid.org/0000-0002-8922-9500; Email: salman.shakil@bracu.ac.bd

Authors

Nazifa Tabassum Tasnim − *Department of Mathematics and Natural Sciences, Brac University, Dhaka 1212, Bangladesh*

Nushrat Ferdous − *Department of Mathematics and Natural Sciences, Brac University, Dhaka 1212, Bangladesh*

Md. Mahamudul Hasan Rumon − *Department of Mathematics and Natural Sciences, Brac University, Dhaka 1212, Bangladesh*

Complete contact information is available at: https://pubs.acs.org/10.1021/acsomega.3c06323

Author Contributions

[‡]N.T.T. and N.F. contributed equally to this work. Conceptualization, M.S.S.; writing—original draft preparation, N.T.T., N.F., M.S.S., M.H.R.; writing—review and editing, M.S.S.; project administration, M.S.S. All authors have read and agreed to the published version of the manuscript.

Notes

The authors declare no competing financial interest.

ACKNOWLEDGMENTS

The authors are thankful to the School of Data and Sciences Course Waiver for Research Policy of Brac University, Bangladesh.

REFERENCES

(1) Tacconelli, E.; Pezzani, M. D. Public health burden of antimicrobial resistance in Europe. *Lancet Infectious Diseases* **2019**, *19* (1), 4−6.

(2) O'Neill, J. *Tackling Drug-Resistant Infections Globally: Final Report and Recommendations*; Government of the United Kingdom, 2016.

(3) Aslam, B.; Wang, W.; Arshad, M. I.; Khurshid, M.; Muzammil, S.; Rasool, M. H.; Nisar, M. A.; Alvi, R. F.; Aslam, M. A.; Qamar, M. U.; Salamat, M. K. F.; Baloch, Z. Antibiotic resistance: a rundown of a global crisis. *Infect Drug Resist* **2018**, *11*, 1645−1658.

(4) Jain, A. S.; Pawar, P. S.; Sarkar, A.; Junnuthula, V.; Dyawanapelly, S. Bionanofactories for Green Synthesis of Silver Nanoparticles: Toward Antimicrobial Applications. *Int. J. Mol. Sci.* **2021**, *22* (21), No. 11993.

(5) Lallo da Silva, B.; Abuçafy, M. P.; Berbel Manaia, E.; Oshiro Junior, J. A.; Chiari-Andréo, B. G.; Pietro, R. C. R.; Chiavacci, L. A. Relationship Between Structure And Antimicrobial Activity Of Zinc Oxide Nanoparticles: An Overview. *Int. J. Nanomedicine* **2019**, *14*, 9395−9410.

(6) Farias, I. A. P.; Dos Santos, C. C. L.; Sampaio, F. C. Antimicrobial Activity of Cerium Oxide Nanoparticles on Opportunistic Microorganisms: A Systematic Review. *Biomed Res. Int.* **2018**, *2018*, No. 1923606.

(7) Mussin, J.; Robles-Botero, V.; Casañas-Pimentel, R.; Rojas, F.; Angiolella, L.; San Martín-Martínez, E.; Giusiano, G. Antimicrobial and cytotoxic activity of green synthesis silver nanoparticles targeting skin and soft tissue infectious agents. *Sci. Rep* **2021**, *11* (1), No. 14566.

(8) Yu, B.; Wang, Z.; Almutairi, L.; Huang, S.; Kim, M. H. Harnessing iron-oxide nanoparticles towards the improved bactericidal activity of macrophage against Staphylococcus aureus. *Nanomedicine* **2020**, *24*, No. 102158.

(9) Hussein, M. Z.; Al Ali, S.; Geilich, B.; El Zowalaty, M.; Webster, T. Synthesis, characterization, and antimicrobial activity of an ampicillin-conjugated magnetic nanoantibiotic for medical applications. *Int. J. Nanomedicine* **2014**, *9*, 3801.

(10) Vazquez-Muñoz, R.; Meza-Villezcas, A.; Fournier, P. G. J.; Soria-Castro, E.; Juarez-Moreno, K.; Gallego-Hernández, A. L.; Bogdanchikova, N.; Vazquez-Duhalt, R.; Huerta-Saquero, A. Enhancement of antibiotics antimicrobial activity due to the silver nanoparticles impact on the cell membrane. *PLoS One* **2019**, *14* (11), No. e0224904.

(11) Arakha, M.; Pal, S.; Samantarrai, D.; Panigrahi, T. K.; Mallick, B. C.; Pramanik, K.; Mallick, B.; Jha, S. Antimicrobial activity of iron oxide nanoparticle upon modulation of nanoparticle-bacteria interface. *Sci. Rep* **2015**, *5*, 14813.

(12) Li, Y.; Ye, D.; Li, M.; Ma, M.; Gu, N. Adaptive Materials Based on Iron Oxide Nanoparticles for Bone Regeneration. *ChemPhysChem* **2018**, *19* (16), 1965−1979.

(13) Das, S.; Diyali, S.; Vinothini, G.; Perumalsamy, B.; Balakrishnan, G.; Ramasamy, T.; Dharumadurai, D.; Biswas, B. Synthesis, morphological analysis, antibacterial activity of iron oxide nanoparticles and the cytotoxic effect on lung cancer cell line. *Heliyon* **2020**, *6* (9), No. e04953.

(14) Wang, G.; Zhang, X.; Skallberg, A.; Liu, Y.; Hu, Z.; Mei, X.; Uvdal, K. One-step synthesis of water-dispersible ultra-small Fe3O4 nanoparticles as contrast agents for T1 and T2 magnetic resonance imaging. *Nanoscale* **2014**, *6* (5), 2953−2963.

(15) Kumar, C. S. S. R.; Mohammad, F. Magnetic nanomaterials for hyperthermia-based therapy and controlled drug delivery. *Adv. Drug Delivery Rev.* **2011**, *63* (9), 789−808.

(16) Al-Brahim, J. S. Saussurea costus extract as bio mediator in synthesis iron oxide nanoparticles (IONPs) and their antimicrobial ability. *PLoS One* **2023**, *18* (3), No. e0282443.

(17) Zhang, N.; Peng, H.; Hu, B. Light-induced pH change and its application to solid phase extraction of trace heavy metals by high-magnetization Fe3O4@SiO2@TiO2 nanoparticles followed by

inductively coupled plasma mass spectrometry detection. *Talanta* **2012**, *94*, 278−283.

(18) Chang, Q.; Huang, J.; Ding, Y.; Tang, H. Catalytic Oxidation of Phenol and 2,4-Dichlorophenol by Using Horseradish Peroxidase Immobilized on Graphene Oxide/Fe3O4. *Molecules* **2016**, *21* (8), 1044.

(19) Xu, C.; Akakuru, O. U.; Zheng, J.; Wu, A. Applications of Iron Oxide-Based Magnetic Nanoparticles in the Diagnosis and Treatment of Bacterial Infections. *Front Bioeng Biotechnol* **2019**, *7*, 141.

(20) Armijo, L. M.; Wawrzyniec, S. J.; Kopciuch, M.; Brandt, Y. I.; Rivera, A. C.; Withers, N. J.; Cook, N. C.; Huber, D. L.; Monson, T. C.; Smyth, H. D. C.; Osiński, M. Antibacterial activity of iron oxide, iron nitride, and tobramycin conjugated nanoparticles against Pseudomonas aeruginosa biofilms. *J. Nanobiotechnology* **2020**, *18* (1), 35.

(21) Samavati, A.; F. Ismail, A. Antibacterial properties of copper-substituted cobalt ferrite nanoparticles synthesized by co-precipitation method. *Particuology* **2017**, *30*, 158−163.

(22) Rekha, K.; Nirmala, M.; Nair, M. G.; Anukaliani, A. Structural, optical, photocatalytic and antibacterial activity of zinc oxide and manganese doped zinc oxide nanoparticles. *Physica B: Condensed Matter* **2010**, *405* (15), 3180−3185.

(23) Laha, S. S.; Thorat, N. D.; Singh, G.; Sathish, C. I.; Yi, J.; Dixit, A.; Vinu, A. Rare-Earth Doped Iron Oxide Nanostructures for Cancer Theranostics: Magnetic Hyperthermia and Magnetic Resonance Imaging. *Small* **2022**, *18* (11), No. 2104855.

(24) Anbu, P. Chemical synthesis of NiFe2O4/NG/cellulose nanocomposite and its antibacterial potential against bacterial pathogens. *Biotechnology and Applied Biochemistry* **2022**, *69* (3), 867−875.

(25) Vijayalakshmi, K.; Noor Ul Haq, L. L, Microwave-sonochemical synergistically assisted synthesis of hybrid Ni-Fe3O4/ZnO nanocomposite for enhanced antibacterial performance. *Mater. Today Commun.* **2021**, *26*, No. 101835.

(26) Raveesha, H. R.; Bharath, H. L.; Vasudha, D. R.; Sushma, B. K.; Pratibha, S.; Dhananjaya, N. Antibacterial and antiproliferation activity of green synthesized nanoparticles from rhizome extract of Alpinia galangal (L.) Wild. *Inorg. Chem. Commun.* **2021**, *132*, No. 108854.

(27) Bhushan, M.; Kumar, Y.; Periyasamy, L.; Viswanath, A. K. Study of synthesis, structural, optical and magnetic characterizations of iron/copper oxide nanocomposites: A promising novel inorganic antibiotic. *Materials Science and Engineering: C* **2019**, *96*, 66−76.

(28) Rahdar, A.; Beyzaei, H.; Saadat, M.; Yu, X.; Trant, J. F. Synthesis, physical characterization, and antifungal and antibacterial activities of oleic acid capped nanomagnetite and cobalt-doped nanomagnetite. *Can. J. Chem.* **2020**, *98* (1), 34−39.

(29) Janczak, K.; Kosmalska, D.; Kaczor, D.; Raszkowska-Kaczor, A.; Wedderburn, L.; Malinowski, R. Bactericidal and Fungistatic Properties of LDPE Modified with a Biocide Containing Metal Nanoparticles. *Materials* **2021**, *14* (15), 4228.

(30) Haghniaz, R.; Rabbani, A.; Vajhadin, F.; Khan, T.; Kousar, R.; Khan, A. R.; Montazerian, H.; Iqbal, J.; Libanori, A.; Kim, H.-J.; Wahid, F. Anti-bacterial and wound healing-promoting effects of zinc ferrite nanoparticles. *J. Nanobiotechnol.* **2021**, *19* (1), 38.

(31) Ahghari, M. R.; Amiri-khamakani, Z.; Maleki, A. Synthesis and characterization of Se doped Fe3O4 nanoparticles for catalytic and biological properties. *Sci. Rep.* **2023**, *13* (1), 1007.

(32) Shujah, T.; Shahzadi, A.; Haider, A.; Mustajab, M.; Haider, A. M.; Ul-Hamid, A.; Haider, J.; Nabgan, W.; Ikram, M. Molybdenum-doped iron oxide nanostructures synthesized via a chemical co-precipitation route for efficient dye degradation and antimicrobial performance: in silico molecular docking studies. *RSC Adv.* **2022**, *12* (54), 35177−35191.

(33) Zhao, X.; Smith, G.; Javed, B.; Dee, G.; Gun'ko, Y. K.; Curtin, J.; Byrne, H. J.; O'Connor, C.; Tian, F. Design and Development of Magnetic Iron Core Gold Nanoparticle-Based Fluorescent Multiplex Assay to Detect Salmonella. *Nanomaterials (Basel)* **2022**, *12* (21), No. 3917.

(34) Žalnėravičius, R.; Mikalauskaitė, A.; Niaura, G.; Paškevičius, A.; Jagminas, A. Ultra-small methionine-capped Au0/Au+ nanoparticles as efficient drug against the antibiotic-resistant bacteria. *Materials Science and Engineering: C* **2019**, *102*, 646−652.

(35) Zhou, W.; Fu, L.; Zhao, L.; Xu, X.; Li, W.; Wen, M.; Wu, Q. Novel Core−Sheath Cu/Cu2O-ZnO-Fe3O4 Nanocomposites with High-Efficiency Chlorine-Resistant Bacteria Sterilization and Trichloroacetic Acid Degradation Performance. *ACS Appl. Mater. Interfaces* **2021**, *13* (9), 10878−10890.

(36) Babu, A. T.; Sebastian, M.; Manaf, O.; Antony, R. Heterostructured Nanocomposites of Ag Doped Fe3O4 Embedded in ZnO for Antibacterial Applications and Catalytic Conversion of Hazardous Wastes. *Journal of Inorganic and Organometallic Polymers and Materials* **2020**, *30* (6), 1944−1955.

(37) Zhu, L.; Pearson, D. W.; Benoit, S. L.; Xie, J.; Pant, J.; Yang, Y.; Mondal, A.; Handa, H.; Howe, J. Y.; Hung, Y. C.; Vidal, J. E.; Maier, R. J.; Zhao, Y. Highly Efficient Antimicrobial Activity of Cu(x)Fe(y)O(z) Nanoparticles against Important Human Pathogens. *Nanomaterials (Basel)* **2020**, *10* (11), No. 2294.

(38) Gudkov, S. V.; Burmistrov, D. E.; Serov, D. A.; Rebezov, M. B.; Semenova, A. A.; Lisitsyn, A. B. Do Iron Oxide Nanoparticles Have Significant Antibacterial Properties? *Antibiotics (Basel)* **2021**, *10* (7), No. 884.

(39) Arias, L. S.; Pessan, J. P.; Vieira, A. P. M.; Lima, T. M. T.; Delbem, A. C. B.; Monteiro, D. R. Iron Oxide Nanoparticles for Biomedical Applications: A Perspective on Synthesis, Drugs, Antimicrobial Activity, and Toxicity. *Antibiotics (Basel)* **2018**, *7* (2), No. 46.

(40) Hamdy, N. M.; Boseila, A. A.; Ramadan, A.; Basalious, E. B. Iron Oxide Nanoparticles-Plant Insignia Synthesis with Favorable Biomedical Activities and Less Toxicity, in the "Era of the-Green": A Systematic Review. *Pharmaceutics* **2022**, *14* (4), No. 844.

(41) Yang, Y.; Liu, Y.; Song, L.; Cui, X.; Zhou, J.; Jin, G.; Boccaccini, A. R.; Virtanen, S. Iron oxide nanoparticle-based nanocomposites in biomedical application. *Trends Biotechnol* **2023**, *41*, 1471.

(42) Figuerola, A.; Di Corato, R.; Manna, L.; Pellegrino, T. From iron oxide nanoparticles towards advanced iron-based inorganic materials designed for biomedical applications. *Pharmacol. Res.* **2010**, *62* (2), 126−143.

(43) Noqta, O. A.; Aziz, A. A.; Usman, I. A.; Bououdina, M. Recent Advances in Iron Oxide Nanoparticles (IONPs): Synthesis and Surface Modification for Biomedical Applications. *Journal of Superconductivity and Novel Magnetism* **2019**, *32* (4), 779−795.

(44) Iriarte-Mesa, C.; López, Y. C.; Matos-Peralta, Y.; de la Vega-Hernández, K.; Antuch, M. Gold, Silver and Iron Oxide Nanoparticles: Synthesis and Bionanoconjugation Strategies Aimed at Electrochemical Applications. *Top Curr. Chem. (Cham)* **2020**, *378* (1), 12.

(45) Tringides, M. C.; Jałochowski, M.; Bauer, E. Quantum size effects in metallic nanostructures. *Phys. Today* **2007**, *60* (4), 50−54.

(46) Trindade, T.; Thomas, P. J. 4.13—Defining and Using Very Small Crystals. In *Comprehensive Inorganic Chemistry II*, 2nd ed.; Reedijk, J., Poeppelmeier, K., Eds.; Elsevier: Amsterdam, 2013; pp 343−369.

(47) Li, Q.; Kartikowati, C. W.; Horie, S.; Ogi, T.; Iwaki, T.; Okuyama, K. Correlation between particle size/domain structure and magnetic properties of highly crystalline Fe3O4 nanoparticles. *Sci. Rep.* **2017**, *7* (1), 9894.

(48) Ajinkya, N.; Yu, X.; Kaithal, P.; Luo, H.; Somani, P.; Ramakrishna, S. Magnetic Iron Oxide Nanoparticle (IONP) Synthesis to Applications: Present and Future. *Materials* **2020**, *13* (20), 4644.

(49) Gawande, M. B.; Goswami, A.; Felpin, F.-X.; Asefa, T.; Huang, X.; Silva, R.; Zou, X.; Zboril, R.; Varma, R. S. Cu and Cu-Based Nanoparticles: Synthesis and Applications in Catalysis. *Chem. Rev.* **2016**, *116* (6), 3722−3811.

(50) Sharma, R. P.; Raut, S. D.; Jadhav, V. V.; Mulani, R. M.; Kadam, A. S.; Mane, R. S. Assessment of antibacterial and anti-biofilm effects of zinc ferrite nanoparticles against *Klebsiella pneumoniae*. *Folia Microbiologica* **2022**, *67* (5), 747−755.

https://doi.org/10.1021/acsomega.3c06323
ACS Omega 2024, 9, 16−32

(51) Adamiano, A.; Wu, V. M.; Carella, F.; Lamura, G.; Canepa, F.; Tampieri, A.; Iafisco, M.; Uskoković, V. Magnetic calcium phosphates nanocomposites for the intracellular hyperthermia of cancers of bone and brain. *Nanomedicine (London, England)* **2019**, *14* (10), 1267–1289.

(52) Sadeghi Rad, T.; Khataee, A.; Vafaei, F.; Rahim Pouran, S. Chromium and cerium co-doped magnetite/reduced graphene oxide nanocomposite as a potent antibacterial agent against *S. aureus*. *Chemosphere* **2021**, *274*, No. 129988.

(53) Kasparis, G.; Sangnier, A. P.; Wang, L.; Efstathiou, C.; LaGrow, A. P.; Sergides, A.; Wilhelm, C.; Thanh, N. T. K. Zn doped iron oxide nanoparticles with high magnetization and photothermal efficiency for cancer treatment. *J. Mater. Chem. B* **2023**, *11* (4), 787–801.

(54) Din, I. U.; Khan, I. S.; Gul, I. H.; Hussain, Z.; Miran, W.; Javaid, F.; Liaqat, U. Novel cytotoxicity study of strontium (Sr) doped iron oxide (Fe(3)O(4)) nanoparticles aided with ibuprofen for drug delivery applications. *Naunyn Schmiedebergs Arch Pharmacol* **2023**, DOI: 10.1007/s00210-023-02582-7.

(55) Shujah, T.; Shahzadi, A.; Haider, A.; Mustajab, M.; Haider, A. M.; Ul-Hamid, A.; Haider, J.; Nabgan, W.; Ikram, M. Molybdenum-doped iron oxide nanostructures synthesized via a chemical co-precipitation route for efficient dye degradation and antimicrobial performance: in silico molecular docking studies. *RSC Adv.* **2022**, *12* (54), 35177–35191.

(56) Park, J. C.; Lee, G. T.; Kim, H. K.; Sung, B.; Lee, Y.; Kim, M.; Chang, Y.; Seo, J. H. Surface Design of Eu-Doped Iron Oxide Nanoparticles for Tuning the Magnetic Relaxivity. *ACS Appl. Mater. Interfaces* **2018**, *10* (30), 25080–25089.

(57) Elayakumar, K.; Dinesh, A.; Manikandan, A.; Palanivelu, M.; Kavitha, G.; Prakash, S.; Thilak Kumar, R.; Jaganathan, S. K.; Baykal, A. Structural, morphological, enhanced magnetic properties and antibacterial bio-medical activity of rare earth element (REE) cerium (Ce^{3+}) doped $CoFe_2O_4$ nanoparticles. *J. Magn. Magn. Mater.* **2019**, *476*, 157–165.

(58) Casula, M. F.; Conca, E.; Bakaimi, I.; Sathya, A.; Materia, M. E.; Casu, A.; Falqui, A.; Sogne, E.; Pellegrino, T.; Kanaras, A. G. Manganese doped-iron oxide nanoparticle clusters and their potential as agents for magnetic resonance imaging and hyperthermia. *Phys. Chem. Chem. Phys.* **2016**, *18* (25), 16848–55.

(59) Dhanakotti, R. B.; Kaliyamoorthy, V.; Mane Prabhu, K. B.; Ravi, S.; Radhakrishnan, V.; Saminathan, M.; Pandurangan, A.; Mukannan, A.; Yasuhiro, H. Structural and magnetic properties of cobalt-doped iron oxide nanoparticles prepared by solution combustion method for biomedical applications. *Int. J. Nanomedicine* **2015**, *10*, 189–98.

(60) Mohtar, S. S.; Aziz, F.; Ismail, A. F.; Sambudi, N. S.; Abdullah, H.; Rosli, A. N.; Ohtani, B. Impact of Doping and Additive Applications on Photocatalyst Textural Properties in Removing Organic Pollutants: A Review. *Catalysts* **2021**, *11* (10), 1160.

(61) Zhang, R.; Zhao, H.; Fan, K. Structure-Activity Mechanism of Iron Oxide Nanozymes. *Nanozymes: Design, Synthesis, and Applications, American Chemical Society* **2022**, *1422*, 1–35.

(62) Shakil, R.; Rumon, M. M. H.; Tarek, Y. A.; Roy, C. K.; Chowdhury, A.-N.; Das, R. Chapter 5—Surface-modified nanomaterials-based catalytic materials for water purification, hydrocarbon production, and pollutant remediation. In *Surface Modified Nanomaterials for Applications in Catalysis*; Gawande, M. B., Mustansar Hussain, C., Yamauchi, Y., Eds.; Elsevier: 2022; pp 103–130.

(63) Mehra, A.; Chamoli, S.; Kumar, N.; Gautam, V.; Shrivastava, P.; Kumar, V.; Verma, P.; Kumar, P.; Maurya, P. K. 12—Catalytically active nanomaterials as artificial enzymes. In *Oxides for Medical Applications*; Kumar, P., Kandasamy, G., Singh, J. P., Maurya, P. K., Eds.; Woodhead Publishing: 2023; pp 305–337.

(64) Shen, Y.; Pan, T.; Wang, L.; Ren, Z.; Zhang, W.; Huo, F. Programmable Logic in Metal–Organic Frameworks for Catalysis. *Adv. Mater.* **2021**, *33* (46), No. 2007442.

(65) Osman, A. I.; Elgarahy, A. M.; Eltaweil, A. S.; Abd El-Monaem, E. M.; El-Aqapa, H. G.; Park, Y.; Hwang, Y.; Ayati, A.; Farghali, M.; Ihara, I.; Al-Muhtaseb, A. a. H.; Rooney, D. W.; Yap, P.-S.; Sillanpää, M. Biofuel production, hydrogen production and water remediation by photocatalysis, biocatalysis and electrocatalysis. *Environmental Chemistry Letters* **2023**, *21* (3), 1315–1379.

(66) Wu, G.; Santandreu, A.; Kellogg, W.; Gupta, S.; Ogoke, O.; Zhang, H.; Wang, H.-L.; Dai, L. Carbon nanocomposite catalysts for oxygen reduction and evolution reactions: From nitrogen doping to transition-metal addition. *Nano Energy* **2016**, *29*, 83–110.

(67) Lei, L.; Huang, D.; Zeng, G.; Cheng, M.; Jiang, D.; Zhou, C.; Chen, S.; Wang, W. A fantastic two-dimensional MoS_2 material based on the inert basal planes activation: Electronic structure, synthesis strategies, catalytic active sites, catalytic and electronics properties. *Coord. Chem. Rev.* **2019**, *399*, No. 213020.

(68) Shi, Z.; Yang, W.; Gu, Y.; Liao, T.; Sun, Z. Metal-Nitrogen-Doped Carbon Materials as Highly Efficient Catalysts: Progress and Rational Design. *Advanced Science* **2020**, *7* (15), No. 2001069.

(69) Samanta, A.; Jana, S. Ni-, Co-, and Mn-Doped Fe_2O_3 Nano-Parallelepipeds for Oxygen Evolution. *ACS Appl. Nano Mater.* **2021**, *4* (5), 5131–5140.

(70) El Maalam, K.; Ben Ali, M.; El Moussaoui, H.; Mounkachi, O.; Hamedoun, M.; Masrour, R.; Hlil, E. K.; Benyoussef, A. Magnetic properties of tin ferrites nanostructures doped with transition metal. *J. Alloys Compd.* **2015**, *622*, 761–764.

(71) Dippong, T.; Levei, E. A.; Cadar, O. Recent Advances in Synthesis and Applications of MFe_2O_4 (M = Co, Cu, Mn, Ni, Zn) Nanoparticles. *Nanomaterials* **2021**, *11* (6), 1560.

(72) Pereira, C.; Pereira, A. M.; Fernandes, C.; Rocha, M.; Mendes, R.; Fernández-García, M. P.; Guedes, A.; Tavares, P. B.; Grenèche, J.-M.; Araújo, J. P.; Freire, C. Superparamagnetic MFe_2O_4 (M = Fe, Co, Mn) Nanoparticles: Tuning the Particle Size and Magnetic Properties through a Novel One-Step Coprecipitation Route. *Chem. Mater.* **2012**, *24* (8), 1496–1504.

(73) Wang, B.; Zhang, X.; Zhang, Y.; Yuan, S.; Guo, Y.; Dong, S.; Wang, J. Prediction of a two-dimensional high-TC f-electron ferromagnetic semiconductor. *Materials Horizons* **2020**, *7* (6), 1623–1630.

(74) Yang, Y.; Fan, X.-L.; Pan, R.; Guo, W.-J. First-principles investigations of transition-metal doped bilayer WS_2. *Phys. Chem. Chem. Phys.* **2016**, *18* (15), 10152–10157.

(75) Liu, Z.; Yu, F.; Dong, D.; Gui, R.; Li, W.; Sun, R.; Wan, Y.; Dan, J.; Wang, Q.; Dai, B. Transition-metal-doped ceria carried on two-dimensional vermiculite for selective catalytic reduction of NO with CO: Experiments and density functional theory. *Appl. Surf. Sci.* **2021**, *566*, No. 150704.

(76) Xie, C.; Sun, Y.; Zhu, B. The promoting mechanism of doping Mn, Co, and Ce on gas adsorption property and anti-SO_2 oxidation over γ-Fe_2O_3 (001) surface: A density functional theory study. *Colloids Surf., A* **2021**, *628*, No. 127218.

(77) Jarlborg, T.; Barbiellini, B.; Lane, C.; Wang, Y. J.; Markiewicz, R. S.; Liu, Z.; Hussain, Z.; Bansil, A. Electronic structure and excitations in oxygen deficient $CeO_{2-\delta}$ from DFT calculations. *Phys. Rev. B* **2014**, *89* (16), No. 165101.

(78) Lu, C.; Xu, X.; Zhang, T.; Wang, Z.; Chai, Y. Facile synthesis of superparamagnetic nickel-doped iron oxide nanoparticles as high-performance T(1) contrast agents for magnetic resonance imaging. *J. Mater. Chem. B* **2022**, *10* (10), 1623–1633.

(79) Das, P.; Salvioni, L.; Malatesta, M.; Vurro, F.; Mannucci, S.; Gerosa, M.; Antonietta Rizzuto, M.; Tullio, C.; Degrassi, A.; Colombo, M.; Ferretti, A. M.; Ponti, A.; Calderan, L.; Prosperi, D. Colloidal polymer-coated Zn-doped iron oxide nanoparticles with high relaxivity and specific absorption rate for efficient magnetic resonance imaging and magnetic hyperthermia. *J. Colloid Interface Sci.* **2020**, *579*, 186–194.

(80) Mehrmohammadi, M.; Shin, T. H.; Qu, M.; Kruizinga, P.; Truby, R. L.; Lee, J. H.; Cheon, J.; Emelianov, S. Y. In vivo pulsed magneto-motive ultrasound imaging using high-performance magnetoactive contrast nanoagents. *Nanoscale* **2013**, *5* (22), 11179–86.

(81) Hsieh, Y. K.; Jiang, P. S.; Yang, B. S.; Sun, T. Y.; Peng, H. H.; Wang, C. F. Using laser ablation/inductively coupled plasma mass

spectrometry to bioimage multiple elements in mouse tumors after hyperthermia. *Anal Bioanal Chem.* **2011**, *401* (3), 909−15.

(82) Dong, S.; Xu, J.; Jia, T.; Xu, M.; Zhong, C.; Yang, G.; Li, J.; Yang, D.; He, F.; Gai, S.; Yang, P.; Lin, J. Upconversion-mediated ZnFe(2)O(4) nanoplatform for NIR-enhanced chemodynamic and photodynamic therapy. *Chem. Sci.* **2019**, *10* (15), 4259−4271.

(83) Tamm, A.; Tarre, A.; Kozlova, J.; Rähn, M.; Jõgiaas, T.; Kahro, T.; Link, J.; Stern, R. Atomic layer deposition of superparamagnetic ruthenium-doped iron oxide thin film. *RSC Adv.* **2021**, *11* (13), 7521−7526.

(84) Das, B.; Girigoswami, A.; Dutta, A.; Pal, P.; Dutta, J.; Dadhich, P.; Srivas, P. K.; Dhara, S. Carbon Nanodots Doped Superparamagnetic Iron Oxide Nanoparticles for Multimodal Bioimaging and Osteochondral Tissue Regeneration via External Magnetic Actuation. *ACS Biomater Sci. Eng.* **2019**, *5* (7), 3549−3560.

(85) Pioletti, D. P. Integration of mechanotransduction concepts in bone tissue engineering. *Comput. Methods Biomech Biomed Engin* **2013**, *16* (10), 1050−5.

(86) Kobayashi, Y.; Hauptmann, R.; Kratz, H.; Ebert, M.; Wagner, S.; Taupitz, M. Europium doping of superparamagnetic iron oxide nanoparticles enables their detection by fluorescence microscopy and for quantitative analytics. *Technology and Health Care* **2017**, *25*, 457−470.

(87) Yang, G.; Su, Q.; Lv, J.; Zheng, Y.; Song, T.; Zhang, H.; Li, M.; Zhou, W.; Li, T.; Qin, X.; Li, S.; Wu, C.; Liao, X.; Liu, Y.; Yang, H. Bio-inspired Oxidative Stress Amplifier for Suppressing Cancer Metastasis and Imaging-Guided Combination Therapy. *ACS Appl. Mater. Interfaces* **2023**, *15* (5), 6572−6583.

(88) Mohammadi, Z.; Attaran, N.; Sazgarnia, A.; Shaegh, S. A. M.; Montazerabadi, A. Superparamagnetic cobalt ferrite nanoparticles as T(2) contrast agent in MRI: in vitro study. *IET Nanobiotechnol* **2020**, *14* (5), 396−404.

(89) Mazarío, E.; Cañete, M.; Herranz, F.; Sánchez-Marcos, J.; de la Fuente, J. M.; Herrasti, P.; Menéndez, N. Highly Efficient T2 Cobalt Ferrite Nanoparticles Vectorized for Internalization in Cancer Cells. *Pharmaceuticals (Basel)* **2021**, *14* (2), No. 124.

(90) Nica, V.; Caro, C.; Páez-Muñoz, J. M.; Leal, M. P.; Garcia-Martin, M. L. Bi-Magnetic Core-Shell CoFe(2)O(4)@MnFe(2)O(4) Nanoparticles for In Vivo Theranostics. *Nanomaterials (Basel)* **2020**, *10* (5), No. 907.

(91) Porru, M.; Morales, M. D. P.; Gallo-Cordova, A.; Espinosa, A.; Moros, M.; Brero, F.; Mariani, M.; Lascialfari, A.; Ovejero, J. G. Tailoring the Magnetic and Structural Properties of Manganese/Zinc Doped Iron Oxide Nanoparticles through Microwaves-Assisted Polyol Synthesis. *Nanomaterials (Basel)* **2022**, *12* (19), No. 3304.

(92) Nowicka, A. M.; Ruzycka-Ayoush, M.; Kasprzak, A.; Kowalczyk, A.; Bamburowicz-Klimkowska, M.; Sikorska, M.; Sobczak, K.; Donten, M.; Ruszczynska, A.; Nowakowska, J.; Grudzinski, I. P. Application of biocompatible and ultrastable superparamagnetic iron(iii) oxide nanoparticles doped with magnesium for efficient magnetic fluid hyperthermia in lung cancer cells. *J. Mater. Chem. B* **2023**, *11* (18), 4028−4041.

(93) Fang, W.; Zhu, W.; Chen, H.; Zhang, H.; Hong, S.; Wei, W.; Zhao, T. MRI Enhancement and Tumor Targeted Drug Delivery Using Zn(2+)-Doped Fe(3)O(4) Core/Mesoporous Silica Shell Nanocomposites. *ACS Appl. Bio Mater.* **2020**, *3* (3), 1690−1697.

(94) Din, I. U.; Khan, I. S.; Gul, I. H.; Hussain, Z.; Miran, W.; Javaid, F.; Liaqat, U. Novel cytotoxicity study of strontium (Sr) doped iron oxide (Fe3O4) nanoparticles aided with ibuprofen for drug delivery applications. *Naunyn-Schmiedeberg's Archives of Pharmacology* **2023**, DOI: 10.1007/s00210-023-02582-7.

(95) Luo, Y.; Zhang, W.; Liao, Z.; Yang, S.; Yang, S.; Li, X.; Zuo, F.; Luo, J. Role of Mn(2+) Doping in the Preparation of Core-Shell Structured Fe_3O_4@upconversion Nanoparticles and Their Applications in T_1/T_2-Weighted Magnetic Resonance Imaging, Upconversion Luminescent Imaging and Near-Infrared Activated Photodynamic Therapy. *Nanomaterials (Basel)* **2018**, *8* (7), No. 466.

(96) Cao, X.; Xia, Z.; Yan, W.; He, S.; Xu, X.; Wei, Z.; Ye, Y.; Zheng, H. Colorimetric biosensing of nopaline synthase terminator using Fe(3)O(4)@Au and hemin-functionalized reduced graphene oxide. *Anal. Biochem.* **2020**, *602*, No. 113798.

(97) Keerthana, S. P.; Yuvakkumar, R.; Ravi, G.; Kumar, P.; Elshikh, M. S.; Alkhamis, H. H.; Alrefaei, A. F.; Velauthapillai, D. A strategy to enhance the photocatalytic efficiency of α-Fe(2)O(3). *Chemosphere* **2021**, *270*, No. 129498.

(98) Babes, L.; Denizot, B. t.; Tanguy, G.; Le Jeune, J. J.; Jallet, P. Synthesis of Iron Oxide Nanoparticles Used as MRI Contrast Agents: A Parametric Study. *J. Colloid Interface Sci.* **1999**, *212* (2), 474−482.

(99) Jolivet, J.-P.; Chanéac, C.; Tronc, E. Iron oxide chemistry. From molecular clusters to extended solid networks. *Chem. Commun.* **2004**, No. 5, 477.

(100) Liu, X.; Ma, Z.; Xing, J.; Liu, H. Preparation and characterization of amino−silane modified superparamagnetic silica nanospheres. *J. Magn. Magn. Mater.* **2004**, *270* (1), 1−6.

(101) Baek, Y. W.; An, Y. J. Microbial toxicity of metal oxide nanoparticles (CuO, NiO, ZnO, and Sb2O3) to Escherichia coli, Bacillus subtilis, and Streptococcus aureus. *Sci. Total Environ.* **2011**, *409* (8), 1603−8.

(102) Hajipour, M. J.; Fromm, K. M.; Akbar Ashkarran, A.; Jimenez de Aberasturi, D.; Larramendi, I. R. d.; Rojo, T.; Serpooshan, V.; Parak, W. J.; Mahmoudi, M. Antibacterial properties of nanoparticles. *Trends Biotechnol* **2012**, *30* (10), 499−511.

(103) Pokhrel, L. R.; Jacobs, Z. L.; Dikin, D.; Akula, S. M. Five nanometer size highly positive silver nanoparticles are bactericidal targeting cell wall and adherent fimbriae expression. *Sci. Rep* **2022**, *12* (1), 6729.

(104) de Lacerda Coriolano, D.; de Souza, J. B.; Bueno, E. V.; Medeiros, S.; Cavalcanti, I. D. L.; Cavalcanti, I. M. F. Antibacterial and antibiofilm potential of silver nanoparticles against antibiotic-sensitive and multidrug-resistant Pseudomonas aeruginosa strains. *Braz J. Microbiol* **2021**, *52* (1), 267−278.

(105) Azam, A.; Ahmed, A. S.; Oves, M.; Khan, M. S.; Habib, S. S.; Memic, A. Antimicrobial activity of metal oxide nanoparticles against Gram-positive and Gram-negative bacteria: a comparative study. *International journal of nanomedicine* **2012**, 6003−6009.

(106) Ismail, R. A.; Sulaiman, G. M.; Abdulrahman, S. A.; Marzoog, T. R. Antibacterial activity of magnetic iron oxide nanoparticles synthesized by laser ablation in liquid. *Mater. Sci. Eng. C Mater. Biol. Appl.* **2015**, *53*, 286−97.

(107) Aruguete, D. M.; Hochella, M. F. Bacteriananoparticle interactions and their environmental implications. *Environmental Chemistry* **2010**, *7* (1), 3−9.

(108) Cabeen, M. T.; Jacobs-Wagner, C. Bacterial cell shape. *Nature Reviews Microbiology* **2005**, *3* (8), 601−610.

(109) Wang, E. C.; Wang, A. Z. Nanoparticles and their applications in cell and molecular biology. *Integrative Biology* **2014**, *6* (1), 9−26.

(110) Rajakumar, G.; Mao, L.; Bao, T.; Wen, W.; Wang, S.; Gomathi, T.; Gnanasundaram, N.; Rebezov, M.; Shariati, M. A.; Chung, I.-M.; Thiruvengadam, M.; Zhang, X. Yttrium Oxide Nanoparticle Synthesis: An Overview of Methods of Preparation and Biomedical Applications. *Applied Sciences* **2021**, *11* (5), 2172.

(111) Saqib, S.; Munis, M. F. H.; Zaman, W.; Ullah, F.; Shah, S. N.; Ayaz, A.; Farooq, M.; Bahadur, S. Synthesis, characterization and use of iron oxide nano particles for antibacterial activity. *Microscopy Research and Technique* **2019**, *82* (4), 415−420.

(112) Al-Shabib, N. A.; Husain, F. M.; Ahmed, F.; Khan, R. A.; Khan, M. S.; Ansari, F. A.; Alam, M. Z.; Ahmed, M. A.; Khan, M. S.; Baig, M. H.; Khan, J. M.; Shahzad, S. A.; Arshad, M.; Alyousef, A.; Ahmad, I. Low Temperature Synthesis of Superparamagnetic Iron Oxide (Fe_3O_4) Nanoparticles and Their ROS Mediated Inhibition of Biofilm Formed by Food-Associated Bacteria. *Frontiers in Microbiology* **2018**, *9*, No. 02567.

(113) Abdulsada, F. M.; Hussein, N. N.; Sulaiman, G. M.; Al Ali, A.; Alhujaily, M. Evaluation of the Antibacterial Properties of Iron Oxide, Polyethylene Glycol, and Gentamicin Conjugated Nanoparticles against Some Multidrug-Resistant Bacteria. *J. Funct Biomater* **2022**, *13* (3), No. 138.

(114) Morais, D. O.; Pancotti, A.; de Souza, G. S.; Saivish, M. V.; Braoios, A.; Moreli, M. L.; Souza, M. V. d. B.; da Costa, V. G.; Wang, J. Synthesis, characterization, and evaluation of antibacterial activity of transition metal oxyde nanoparticles. *J. Mater. Sci.: Mater. Med.* **2021**, *32* (9), 101.

(115) Lima, D. R.; Jiang, N.; Liu, X.; Wang, J.; Vulcani, V. A. S.; Martins, A.; Machado, D. S.; Landers, R.; Camargo, P. H. C.; Pancotti, A. Employing Calcination as a Facile Strategy to Reduce the Cytotoxicity in $CoFe_2O_4$ and $NiFe_2O_4$ Nanoparticles. *ACS Appl. Mater. Interfaces* **2017**, *9* (45), 39830−39838.

(116) Qi, J.; Lan, H.; Liu, R.; Liu, H.; Qu, J. Efficient Microcystis aeruginosa removal by moderate photocatalysis-enhanced coagulation with magnetic Zn-doped Fe_3O_4 particles. *Water Res.* **2020**, *171*, No. 115448.

(117) Ivashchenko, O.; Lewandowski, M.; Peplińska, B.; Jarek, M.; Nowaczyk, G.; Wiesner, M.; Załęski, K.; Babutina, T.; Warowicka, A.; Jurga, S. Synthesis and characterization of magnetite/silver/antibiotic nanocomposites for targeted antimicrobial therapy. *Mater. Sci. Eng. C Mater. Biol. Appl.* **2015**, *55*, 343−59.

(118) Ivashchenko, O.; Woźniak, A.; Coy, E.; Peplinska, B.; Gapinski, J.; Jurga, S. Release and cytotoxicity studies of magnetite/Ag/antibiotic nanoparticles: An interdependent relationship. *Colloids Surf. B Biointerfaces* **2017**, *152*, 85−94.

(119) AlMatar, M.; Makky, A. E.; Var, I.; Koksal, F. The Role of Nanoparticles in the Inhibition of Multidrug-Resistant Bacteria and Biofilms. *Curr. Drug Delivery* **2018**, *15* (4), 470−484.

(120) Kohanski, M. A.; DePristo, M. A.; Collins, J. J. Sublethal antibiotic treatment leads to multidrug resistance via radical-induced mutagenesis. *Mol. Cell* **2010**, *37* (3), 311−20.

(121) Groiss, S.; Selvaraj, R.; Varadavenkatesan, T.; Vinayagam, R. Structural characterization, antibacterial and catalytic effect of iron oxide nanoparticles synthesised using the leaf extract of Cynometra ramiflora. *J. Mol. Struct.* **2017**, *1128*, 572−578.

(122) Koduru, J. R.; Kailasa, S. K.; Bhamore, J. R.; Kim, K.-H.; Dutta, T.; Vellingiri, K. Phytochemical-assisted synthetic approaches for silver nanoparticles antimicrobial applications: A review. *Adv. Colloid Interface Sci.* **2018**, *256*, 326−339.

(123) Janani, B.; Al-Mohaimeed, A. M.; Raju, L. L.; Al Farraj, D. A.; Thomas, A. M.; Khan, S. S. Synthesis and characterizations of hybrid PEG-Fe_3O_4 nanoparticles for the efficient adsorptive removal of dye and antibacterial, and antibiofilm applications. *Journal of Environmental Health Science and Engineering* **2021**, *19* (1), 389−400.

(124) Rayman, M. P. The importance of selenium to human health. *lancet* **2000**, *356* (9225), 233−241.

(125) Vijayalakshmi, K.; Noor Ul Haq, L. Microwave-sonochemical synergistically assisted synthesis of hybrid Ni-Fe_3O_4/ZnO nanocomposite for enhanced antibacterial performance. *Mater. Today Commun.* **2021**, *26*, No. 101835.

(126) Feng, X.; Guo, H.; Patel, K.; Zhou, H.; Lou, X. High performance, recoverable Fe_3O_4ZnO nanoparticles for enhanced photocatalytic degradation of phenol. *Chem. Eng. J.* **2014**, *244*, 327−334.

(127) Ansari, S. A.; Khan, M. M.; Ansari, M. O.; Lee, J.; Cho, M. H. Biogenic Synthesis, Photocatalytic, and Photoelectrochemical Performance of Ag−ZnO Nanocomposite. *J. Phys. Chem. C* **2013**, *117* (51), 27023−27030.

(128) Bell, A. M. T.; Smith, J. N. B.; Attfield, J. P.; Rawson, J. M.; Shankland, K.; David, W. I. F. A synchrotron X-ray powder diffraction study of 4-(2,3,4-trifluorophenyl)-1,2,3,5-dithiadiazolyl. Crystal structure determination using a global optimization method. *New J. Chem.* **1999**, *23* (6), 565−567.

(129) Yu, J.; Zhang, W.; Li, Y.; Wang, G.; Yang, L.; Jin, J.; Chen, Q.; Huang, M. Synthesis, characterization, antimicrobial activity and mechanism of a novel hydroxyapatite whisker/nano zinc oxide biomaterial. *Biomedical Materials* **2015**, *10* (1), No. 015001.

(130) Vedernikova, I. A. Magnetic nanoparticles: Advantages of using, methods for preparation, characterization, application in pharmacy. *Review Journal of Chemistry* **2015**, *5* (3), 256−280.

(131) Plaper, A.; Jenko-Brinovec, S.; Premzl, A.; Kos, J.; Raspor, P. Genotoxicity of trivalent chromium in bacterial cells. Possible effects on DNA topology. *Chem. Res. Toxicol.* **2002**, *15* (7), 943−9.

(132) Božić, L.; Malinović, M.; Gajić, D.; Vračević, S.; Pržulj, S.; Jelić, D.; Šmitran, A. Study of Iron Oxide Nanoparticles Doped with Copper: Antimicrobal and Photocatalytical Activity. *Contemporary Materials* **2020**, DOI: 10.7251/comen2002093j.

(133) Li, Y.; Yang, D.; Wang, S.; Li, C.; Xue, B.; Yang, L.; Shen, Z.; Jin, M.; Wang, J.; Qiu, Z. The Detailed Bactericidal Process of Ferric Oxide Nanoparticles on E. coli. *Molecules* **2018**, *23* (3), 606.

(134) Gabrielyan, L.; Hovhannisyan, A.; Gevorgyan, V.; Ananyan, M.; Trchounian, A. Antibacterial effects of iron oxide (Fe_3O_4) nanoparticles: distinguishing concentration-dependent effects with different bacterial cells growth and membrane-associated mechanisms. *Appl. Microbiol. Biotechnol.* **2019**, *103* (6), 2773−2782.

(135) Padwal, P.; Bandyopadhyaya, R.; Mehra, S. Polyacrylic Acid-Coated Iron Oxide Nanoparticles for Targeting Drug Resistance in Mycobacteria. *Langmuir* **2014**, *30* (50), 15266−15276.

(136) Nallathamby, P. D.; Lee, K. J.; Desai, T.; Xu, X.-H. N. Study of the Multidrug Membrane Transporter of Single Living Pseudomonas aeruginosa Cells Using Size-Dependent Plasmonic Nanoparticle Optical Probes. *Biochemistry* **2010**, *49* (28), 5942−5953.

(137) Choi, O.; Deng, K. K.; Kim, N.-J.; Ross, L.; Surampalli, R. Y.; Hu, Z. The inhibitory effects of silver nanoparticles, silver ions, and silver chloride colloids on microbial growth. *Water Res.* **2008**, *42* (12), 3066−3074.

(138) Dibrov, P.; Dzioba, J.; Gosink, K. K.; Häse, C. C. Chemiosmotic Mechanism of Antimicrobial Activity of Ag^+ in *Vibrio cholerae. Antimicrob. Agents Chemother.* **2002**, *46* (8), 2668−2670.

(139) Almontasser, A.; Parveen, A. Probing the effect of Ni, Co and Fe doping concentrations on the antibacterial behaviors of MgO nanoparticles. *Sci. Rep* **2022**, *12* (1), 7922.

(140) Torres-Mendieta, R.; Nguyen, N. H. A.; Guadagnini, A.; Semerad, J.; Łukowiec, D.; Parma, P.; Yang, J.; Agnoli, S.; Sevcu, A.; Cajthaml, T.; Cernik, M.; Amendola, V. Growth suppression of bacteria by biofilm deterioration using silver nanoparticles with magnetic doping. *Nanoscale* **2022**, *14* (48), 18143−18156.

(141) Tsogoo, A.; Tsedev, N.; Gibaud, A.; Daniel, P.; Kassiba, A.; Fukuda, M.; Kusano, Y.; Azuma, M.; Tsogbadrakh, N.; Ragchaa, G.; Dashzeveg, R.; Ganbold, E.-O. Experimental and ab initio studies on the structural, magnetic, photocatalytic, and antibacterial properties of Cu-doped ZnO nanoparticles. *RSC Adv.* **2023**, *13* (2), 1256−1266.

(142) Rahmati, Z.; Abdi, J.; Vossoughi, M.; Alemzadeh, I. Ag-doped magnetic metal organic framework as a novel nanostructured material for highly efficient antibacterial activity. *Environ. Res.* **2020**, *188*, No. 109555.

(143) Zaman, Y.; Ishaque, M. Z.; Yousaf, Y.; Shahzad, M.; Siddique, A. B.; Arshad, M. I.; Sajid, M.; Ali, N.; Nabi, G. Physical properties of multifunctional TM-doped ZnO nanorods and their photocatalytic and anti-bacterial activities. *Environmental Science and Pollution Research* **2023**, *30* (42), 95860−95874.

(144) Kayani, Z. N.; Kamran, A.; Saddiqe, Z.; Riaz, S.; Naseem, S. Probe of ZrTiO2 thin films with TiO_2-ZrO_2 binary oxides deposited by dip coating technique. *Journal of Photochemistry and Photobiology B: Biology* **2018**, *183*, 357−366.

(145) Özdemir, H.; Faruk Öksüzömer, M. A. Synthesis of Al_2O_3, MgO and $MgAl_2O_4$ by solution combustion method and investigation of performances in partial oxidation of methane. *Powder Technol.* **2020**, *359*, 107−117.

(146) Vindhya, P. S.; Suresh, S.; Kunjikannan, R.; Kavitha, V. T. Antimicrobial, antioxidant, cytotoxicity and photocatalytic performance of Co doped ZnO nanoparticles biosynthesized using *Annona muricata* leaf extract. *Journal of Environmental Health Science and Engineering* **2023**, *21* (1), 167−185.

(147) Kailasa, S. K.; Koduru, J. R. Perspectives of magnetic nature carbon dots in analytical chemistry: From separation to detection and bioimaging. *Trends in Environmental Analytical Chemistry* **2022**, *33*, No. e00153.

(148) Zhu, M.; Zhang, Z.; Zhong, M.; Tariq, M.; Li, Y.; Li, W.; Jin, H.; Skotnicova, K.; Li, Y. Oxygen vacancy induced ferromagnetism in Cu-doped ZnO. *Ceram. Int.* **2017**, *43* (3), 3166−3170.

(149) Liang, Y.; Wang, M.; Zhang, Z.; Ren, G.; Liu, Y.; Wu, S.; Shen, J. Facile synthesis of ZnO QDs@GO-CS hydrogel for synergetic antibacterial applications and enhanced wound healing. *Chem. Eng. J.* **2019**, *378*, No. 122043.

(150) Quan, K.; Zhang, Z.; Chen, H.; Ren, X.; Ren, Y.; Peterson, B. W.; van der Mei, H. C.; Busscher, H. J. Artificial Channels in an Infectious Biofilm Created by Magnetic Nanoparticles Enhanced Bacterial Killing by Antibiotics. *Small* **2019**, *15* (39), No. e1902313.

(151) Karthik, K.; Dhanuskodi, S.; Gobinath, C.; Prabukumar, S.; Sivaramakrishnan, S. Fabrication of MgO nanostructures and its efficient photocatalytic, antibacterial and anticancer performance. *Journal of Photochemistry and Photobiology B: Biology* **2019**, *190*, 8−20.

(152) Yang, Y.; Wang, C.; Wang, N.; Li, J.; Zhu, Y.; Zai, J.; Fu, J.; Hao, Y. Photogenerated reactive oxygen species and hyperthermia by Cu_3SnS_4 nanoflakes for advanced photocatalytic and photothermal antibacterial therapy. *J. Nanobiotechnol.* **2022**, *20* (1), 195.

(153) Krishnan, A.; Vishwanathan, P. V.; Mohan, A. C.; Panchami, R.; Viswanath, S.; Krishnan, A. V. Tuning of Photocatalytic Performance of CeO_2-Fe_2O_3 Composite by Sn-doping for the Effective Degradation of Methlene Blue (MB) and Methyl Orange (MO) dyes. *Surfaces and Interfaces* **2021**, *22*, No. 100808.

(154) Nguyen, T. N. L.; Do, T. V.; Nguyen, T. V.; Dao, P. H.; Trinh, V. T.; Mac, V. P.; Nguyen, A. H.; Dinh, D. A.; Nguyen, T. A.; Vo, T. K. A.; Tran, D. L.; Le, T. L. Antimicrobial activity of acrylic polyurethane/Fe_3O_4-Ag nanocomposite coating. *Prog. Org. Coat.* **2019**, *132*, 15−20.

(155) Kozenkova, E.; Levada, K.; Efremova, M. V.; Omelyanchik, A.; Nalench, Y. A.; Garanina, A. S.; Pshenichnikov, S.; Zhukov, D. G.; Lunov, O.; Lunova, M.; Kozenkov, I.; Innocenti, C.; Albino, M.; Abakumov, M. A.; Sangregorio, C.; Rodionova, V. Multifunctional Fe_3O_4-Au Nanoparticles for the MRI Diagnosis and Potential Treatment of Liver Cancer. *Nanomaterials* **2020**, *10* (9), 1646.

(156) Maiti, D.; Saha, A.; Devi, P. S. Surface modified multifunctional $ZnFe_2O_4$ nanoparticles for hydrophobic and hydrophilic anticancer drug molecule loading. *Phys. Chem. Chem. Phys.* **2016**, *18* (3), 1439−50.

(157) Griffitt, R. J.; Luo, J.; Gao, J.; Bonzongo, J. C.; Barber, D. S. Effects of particle composition and species on toxicity of metallic nanomaterials in aquatic organisms. *Environ. Toxicol. Chem.* **2008**, *27* (9), 1972−8.

(158) Alharby, H. F.; Ali, S. Combined Role of Fe Nanoparticles (Fe NPs) and *Staphylococcus aureus L.* in the Alleviation of Chromium Stress in Rice Plants. *Life (Basel)* **2022**, *12* (3), No. 338, DOI: 10.3390/life12030338.

(159) Wang, J.; Zhu, X.; Zhang, X.; Zhao, Z.; Liu, H.; George, R.; Wilson-Rawls, J.; Chang, Y.; Chen, Y. Disruption of zebrafish (*Danio rerio*) reproduction upon chronic exposure to TiO_2 nanoparticles. *Chemosphere* **2011**, *83* (4), 461−7.

(160) Xia, T.; Wang, J.; Wu, C.; Meng, F.; Shi, Z.; Lian, J.; Feng, J.; Meng, J. Novel complex-coprecipitation route to form high quality triethanolamine-coated Fe_3O_4 nanocrystals: Their high saturation magnetizations and excellent water treatment properties. *CrystEngComm* **2012**, *14* (18), 5741−5744.

(161) Akhtar, K.; Javed, Y.; Muhammad, F.; Akhtar, B.; Shad, N. A.; Sajid, M. M.; Jamil, Y.; Sharif, A.; Abbas, W. Biotransformation and toxicity evaluation of functionalized manganese doped iron oxide nanoparticles. *J. Biomed Mater. Res. B Appl. Biomater* **2021**, *109* (10), 1563−1577.

(162) Acar, M.; Solak, K.; Yildiz, S.; Unver, Y.; Mavi, A. Comparative heating efficiency and cytotoxicity of magnetic silica nanoparticles for magnetic hyperthermia treatment on human breast cancer cells. *3Biotech* **2022**, *12* (11), 313.

(163) Shakil, M. S.; Hasan, M. A.; Uddin, M. F.; Islam, A.; Nahar, A.; Das, H.; Khan, M. N. I.; Dey, B. P.; Rokeya, B.; Hoque, S. M. In Vivo Toxicity Studies of Chitosan-Coated Cobalt Ferrite Nanocomplex for Its Application as MRI Contrast Dye. *ACS Appl. Bio Mater.* **2020**, *3* (11), 7952−7964.

(164) Mngadi, S. M.; Mokhosi, S. R.; Singh, M. Surface-coating of $Mg_{0.5}Co_{0.5}Fe_2O_4$ nanoferrites and their in vitro cytotoxicity. *Inorg. Chem. Commun.* **2019**, *108*, No. 107525.